

**ZONGULDAK BÜLENT ECEVİT UNIVERSITY
GRADUATE SCHOOL OF NATURAL AND APPLIED SCIENCES**

**LONG TIME VARIATION CHARACTERISTICS OF MULTIPATH FROM GPS
AND GLONASS OBSERVATIONS**



DEPARTMENT OF GEOMATIC ENGINEERING

MASTER OF SCIENCE THESIS

TUĞBA KORKMAZ

JULY 2019

**ZONGULDAK BÜLENT ECEVİT UNIVERSITY
GRADUATE SCHOOL OF NATURAL AND APPLIED SCIENCES**

**LONG TIME VARIATION CHARACTERISTICS OF MULTIPATH FROM GPS
AND GLONASS OBSERVATIONS**

DEPARTMENT OF GEOMATIC ENGINEERING

MASTER OF SCIENCE THESIS

TUĞBA KORKMAZ

ADVISOR: Assist. Prof. Kurtuluş Sedar GÖRMÜŞ

ZONGULDAK

July 2019

APPROVAL OF THE THESIS:

The thesis entitled “Long Time Variation Characteristics of Multipath From GPS and GLONASS Observations” and submitted by Tuğba KORKMAZ has been examined and accepted by the jury as a Master of Science thesis in Department of Geomatics Engineering, Graduate School of Natural and Applied Sciences, Zonguldak Bülent Ecevit University 03/07/2019.

Advisor: Assist. Prof. Kurtuluş Sedar GÖRMÜŞ
Zonguldak Bülent Ecevit University, Faculty of Engineering, Department of Geomatics Engineering



Member: Assoc. Prof. Ayhan ATEŞOĞLU
Bartın University, Faculty of Engineering, Department of Forest Engineering



Member: Assist. Prof. Hüseyin KEMALDERE
Zonguldak Bülent Ecevit University, Faculty of Engineering, Department of Geomatics Engineering



Approved by the Graduate School of Natural and Applied Sciences.

..../..../2019



Prof. Ahmet ÖZARSLAN
Director

“With this thesis it is declared that all the information in this thesis is obtained and presented according to academic rules and ethical principles. Also as required by academic rules and ethical principles all works that are not result of this study are cited properly.”


Tuğba KORKMAZ

ABSTRACT

Master of Science Thesis

LONG TIME VARIATION CHARACTERISTICS OF MULTIPATH FROM GPS AND GLONASS OBSERVATIONS

Tuğba KORKMAZ

**Zonguldak Bülent Ecevit University
Graduate School of Natural and Applied Sciences
Department of Geomatic Engineering**

**Thesis Advisor: Assist. Prof. Kurtuluş Sedar GÖRMÜŞ
July 2019, 75 pages**

Global Navigation Satellite Systems (GNSS) that consist of GPS, GLONASS, BeiDou, QZSS, and Galileo have been widely used in navigation, positioning, geodesy, attitude determination, engineering survey and agricultural applications. A number of random and systematic errors like ionospheric delay, tropospheric delay, receiver noise and multipath affect GNSS observations. Most of these errors can be removed by differential techniques. However, multipath delays are independent of each receiver, which cannot be removed by difference. Therefore, multipath is a major error source in differential GNSS positioning. A number of techniques, e.g., notably narrow correlator technology and filtering, have been developed to mitigate multipath errors. In this thesis, the multipath of GPS and GLONASS are estimated and investigated using the linear combinations for both pseudo-ranges P_1 and P_2 and carrier phases L_1 and L_2 data with eliminating the effect of receiver and satellite clocks as well as the atmospheric delay from 3-year (2014-2016) GPS and GLONASS observables at 5 stations. These stations are respectively, DJIG station in Djibouti, DYNG station in Greece, MAL2 station in Kenya, MAYG station in Mayotte and SEYG station in Seychelles.

ABSTRACT (continued)

Results are obtained in different years based on the multipath results and analysis. In 2014, the RMS-MP1 and RMS-MP2 values of the DYNG station were below the decimeter level in both systems. For the SEYG station, the RMS-MP1 value of GLONASS has a small multipath level of 0.02 meters, while the RMS values of GPS shows the highest multipath level of 0.14 meters. In 2015, the smallest RMS-MP1 value is the DYNG and the DJIG stations. The larger effect is the MAL2 station for the RMS-MP1 values of both systems. In 2016, the most affected station is the DJIG station. These multipath are the most related to the surrounding environments of the antenna.

Keywords: GNSS, GPS, GLONASS, Multipath.

Science Code: 616.01.00

ÖZET

Yüksek Lisans Tezi

GPS VE GLONASS GÖZLEMLERİNDEN ÇOKLU DEĞİŞİM ÖZELLİKLERİ

Tuğba KORKMAZ

**Zonguldak Bülent Ecevit Üniversitesi
Fen Bilimleri Enstitüsü
Geomatik Mühendisliği Anabilim Dalı**

Tez Danışmanı: Dr. Öğr. Üyesi Kurtuluş Sedar GÖRMÜŞ

Temmuz 2019, 75 sayfa

GPS, GLONASS, BeiDou, QZSS ve Galileo'dan oluşan Küresel Navigasyon Uydu Sistemleri (GNSS) navigasyon, konum belirleme, jeodezi, davranış belirleme, mühendislik ölçmesi ve tarımsal uygulamalarda yaygın olarak kullanılmaktadır. GNSS ölçümlerini iyonosferik gecikme, troposferik gecikme, alıcı gürültüsü ve çok yolluluk gibi birtakım rastgele ve sistematik hatalar etkilemektedir. Bu hataların çoğu diferansiyel tekniklerle giderilebilir. Ancak, çok yollu gecikmeler, her bir alıcıdan bağımsızdır ve farkla giderilemez. Bu nedenle, çok yolluluk hatası diferansiyel GNSS konum belirlemede büyük bir hata kaynağıdır. Bu hatayı azaltmak için dar korelasyon teknolojisi ve filtreleme gibi birçok teknik geliştirilmiştir. Bu tez çalışmasında, GPS ve GLONASS'ın çok yolluluk hatası, uydu-alıcı saat hatalarının, atmosferik gecikmelerinin etkilerini elimine eden P_1 , P_2 sözde uzunlukların ve L_1 , L_2 taşıyıcı fazların doğrusal kombinasyonları kullanılarak 2014 ve 2016 yılları içinde 5 istasyon üzerinde araştırıldı ve değerlendirildi. Bu istasyonlar sırasıyla Djibouti ülkesinde bulunan DJIG, Yunanistan ülkesinde bulunan DYNG, Kenya ülkesinde bulunan MAL2, Mayotte ülkesinde bulunan MAYG ve Seychelles ülkesinde bulunan SEYG istasyonudur. Uygulama sonucunda farklı yıllara ait çok yolluluk sonuçları ve analizleri elde edildi. 2014 yılında, DYNG

ÖZET (devam ediyor)

istasyonunun RMS-MP1 ve RMS-MP2 değerleri her iki sistemde de desimetre seviyesinin altındadır. SEYG istasyonu için, GLONASS RMS-MP1 değeri 0,02 metre büyüklüğünde en küçük çok yolluluk hatasına sahipken, GPS RMS değerleri 0,14 metre büyüklüğünde en yüksek çok yolluluk hatasına sahiptir. 2015 yılında, en küçük RMS-MP1 değerine DYNG ve DJIG istasyonları sahiptir. Her iki sistemdeki en büyük RMS-MP1 değeri ise MAL2 istasyonudur. 2016 yılında, en çok etkilenen istasyon DJIG istasyonudur. Bu çok yolluluk hatası, en çok istasyon anteninin bulunduğu topografyaya birinci dereceden bağlı olduğu sonucuna varılmaktadır.

Anahtar Kelimeler: GNSS, GPS, GLONASS, Çok Yolluluk Hatası

Bilim Kodu: 616.01.00.

ACKNOWLEDGEMENTS

In the realization of this study, I would like to express my endless thanks and best regards to Assist. Prof. Kurtuluř Sedar GÖRMÜŐ who is my respectable advisor sharing with me his valuable information during the time of the thesis; to Dear Prof. Dr. Őenol Hakan KUTOĐLU who is the Dean of Faculty of Engineering and never hesitate to show his interest; to Dear Prof. Dr. Shuanggen JIN who was a lecturer at the Geomatics Engineering Department in a certain period of the university for his guidance; to Research Assoc. Gökhan GÜRBÜZ who is always with me whenever I have encountered a problem; to Research Assoc. Volkan AKGÜL for his help and support in this way.

Finally, I would like to express my sincere gratitude to my dear family for their support in every period of my life and I also would like to thank my sister Sema KORKMAZ who faced all my difficulties with me during the study.



TABLE OF CONTENTS

	<u>Page</u>
APPROVAL OF THE THESIS:	ii
ABSTRACT	iii
ÖZET	v
ACKNOWLEDGEMENTS	vii
TABLE OF CONTENTS	ix
LIST OF FIGURES	xi
LIST OF TABLES	xiii
LIST OF APPENDICES	xv
LIST OF SYMBOLS AND ABBREVIATIONS	xvii
CHAPTER 1 INTRODUCTION AND OVERVIEW	1
1.1 BACKGROUND	1
1.2 RECENT PROGRESS AND PROBLEMS	2
1.2.1 Progress	2
1.2.2 Motivation	2
1.3 MAIN CONTENT	4
CHAPTER 2 MULTIPATH ESTIMATION	7
2.1 GNSS OBSERVATIONS EQUATIONS	7
2.1.1 Code Observations	7
2.1.2 Carrier Phase Observations	12
2.2 MULTIPATH DELAY	15
2.3 MULTIPATH ESTIMATION	20

TABLE OF CONTENTS (continued)

	<u>Page</u>
CHAPTER 3 RESULTS AND ANALYSIS	25
3.1 MULTIPATH TIME SERIES	26
3.2. STATISTIC ANALYSIS	34
CHAPTER 4 POSITIONAL CHANGES	39
4.1. RESULTS	42
CHAPTER 5 CONCLUSIONS AND DISCUSSION	55
REFERENCES.....	61
APPENDICES	67
CURRICULUM VITAE	75

LIST OF FIGURES

<u>No</u>	<u>Page</u>
Figure 1.1. Processed stations.	5
Figure 2.1. Phase Display	12
Figure 2.2. GNSS multipath model.	16
Figure 2.3. Forward scattering geometry (F-mode).	17
Figure 2.4. Backscattering geometry (B-mode).	18
Figure 2.5. Combined Geometry (C-mode).	19
Figure 3.1. Multipath time-series	27
Figure 3.2. The negative effects of the multipath on the multipath time-series of DJIG station.	28
Figure 3.3. DJIG station (IGS) with Dorne Margolin and choke rings.	28
Figure 3.4. Fluctuations in the multipath time-series of DYNG station.	29
Figure 3.5. The southwest view of the receiver of DYNG station.	30
Figure 3.6. DYNG (EUREF) station with Dorne Margolin and choke rings antenna.	30
Figure 3.7. The multipath time-series of MAL2 station.	31
Figure 3.8. The negative effects of the multipath on the multipath time-series of MAL2 station.	32
Figure 3.9. MAL2 (IGS) station with Dorne Margolin and 3D choke ring antenna.	32
Figure 3.10. The negative effects of the multipath on the multipath time-series of MAYG station.	33
Figure 3.11. MAYG (IGS) station with Dorne Margolin and choke rings.	33
Figure 3.12. The negative effects of the multipath on the multipath time-series of SEYG station.	34
Figure 3.13. RMS-MP1 and RMS-MP2 values of all stations in both systems.	35
Figure 3.14. The RMS-MP1 statistics for all stations.	36
Figure 3.15. The RMS-MP2 statistics for all stations.	37
Figure 4.1. Formed geodetic network.	39
Figure 4.2. Tectonic plates of the selected stations.	42
Figure 4.3. Multipath time-series of the east, north and up components belonging to DJIG station.	43
Figure 4.4. Multipath time-series of the east, north and up components belonging to DYNG station.	44

LIST OF FIGURES (continued)

<u>No</u>	<u>Page</u>
Figure 4.5. Multipath time-series of the east, north and up components belonging to MAL2 station.....	44
Figure 4.6. Multipath time-series of east, north and up components in 2015 and 2016 belonging to MAYG station.	45
Figure 4.7. Multipath time-series of east, north and up components in 2016 belonging to MAYG station.	45
Figure 4.8. Multipath time-series of east, north and up components of SEYG station.....	46
Figure 4.9. Days of the highest multipath values in the multipath time-series graph of the DJIG station.....	47
Figure 4.10. The multipath graph of DJIG station at IGS Network Site Page and high RMS value in the RMS table of the DJIG station.....	47
Figure 4.11. The multipath graph of DJIG station at IGS Network Site Page and high RMS value in the RMS table of the DJIG station.....	48
Figure 4.12. The panoramic view around the receiver of the DYNG station.	48
Figure 4.13. The multipath graph of DYNG station at IGS Network Site Page and high RMS value in the RMS table of the DYNG station.....	49
Figure 4.14. Days of the highest multipath values in the multipath time-series graph of the MAL2 station.....	49
Figure 4.15. The presence of the reflective surfaces around the receiver of the MAL2 station.....	50
Figure 4.16. The residuals graph of MAL2 station at IGS Network Site Page.....	50
Figure 4.17. Days of the highest multipath values in the multipath time-series graph of the MAYG station in 2015 and 2016.....	51
Figure 4.18. Days of the highest multipath values in the multipath time-series graph of the MAYG station in 2016.....	51
Figure 4.19. East and south view around the receiver of the MAYG station.	52
Figure 4.20. West and north view around the receiver of the MAYG station.	52
Figure 4.21. Days of the highest multipath values in the multipath time-series graph of the SEYG station.....	53
Figure 4.22. The residuals graph of SEYG station at IGS Network Site Page.	54
Figure 5.1. Some kind of reflective surfaces around the receiver of DYNG station.	57
Figure 5.2. Time-series graph of DJIG station obtained by GAMIT software.	59

LIST OF TABLES

<u>No</u>	<u>Page</u>
Table 3.1. Nominal satellite signal characteristics	26
Table 3.2. The changes made on DJIG station at IGS network site page.	29
Table 3.3. RMS Table.	31
Table 3.4. Sample trend analysis of DJIG station.	35
Table 3.5. The RMS-MP1 and RMS-MP2 values in meters.....	35
Table 4.1. Tables folder input data.....	40
Table 4.2. GAMIT evaluation strategy.	41



LIST OF APPENDICES

<u>No</u>	<u>Page</u>
Appendix A: RMS Data of GPS in 2014	67





LIST OF SYMBOLS AND ABBREVIATIONS

SYMBOLS

P_1, P_2, P_{L1}, P_{L2}	: Dual-frequency pseudo-range observations
$L_1, L_2, \Phi_{L1}, \Phi_{L2}$: Dual-frequency carrier phase observations
Λ_{L1}	: Wavelength of the signals on L_1
Λ_{L2}	: Wavelength of the signals on L_2
f_1	: Frequency of the signal on L_1
f_2	: Frequency of the signal on L_2
α	: $(f_1 / f_2)^2$
m_1, m_2	: Dual-frequency carrier phase multipath
$MP_{\phi L1}, MP_{\phi L2}$: Carrier phase multipath
M_i	: Pseudo-range multipath for frequency
MP_{L1}, MP_{L2}	: Pseudo-range multipath
MP_1, MP_2	: The pseudo-range multipath effect
B_i, b_1	: Ambiguity bias
n_1, n_2, N_{L1}, N_{L2}	: Integer ambiguities
R	: Geometric distance between the satellite and the receiver
c	: Constant speed of light
Δt^k	: Satellite clock correction
Δt_i	: Receiver clock correction
I_{L1}, I_{L2}	: Ionospheric range errors
T	: Tropospheric range error
$\Delta\Delta$: Double delta
$t_a(t)$: GPS time at which the signal reaches the receiver
$t_u(t)$: GPS time at the exit from the satellite
$t_a^u(t)$: Signal path time
$c[t_a(t) - t_u(t)], \rho_a^u(t)$: The actual geometric distance between the satellite and receiver
$\rho_a^u(t), t_a^u(t)$: The actual signal travel time

LIST OF SYMBOLS AND ABBREVIATIONS (continued)

$\delta_{tu}(t)$: Difference between the satellite clock and the GPS time
$\delta_{ta}(t)$: Difference between the receiver clock time and the GPS time
$P_a^u(t)$: Pseudo-range
$I_a^u(t, f), I_r^s$: Ionospheric effect
$T_a^u(t), T_r^s$: Tropospheric effect
$M_a^u(t)$: Other effects
$\varepsilon_a^u(t)$: Thermal measurements noise and other unmeasurable effects
δ_r	: Receiver hardware delay
δ^s	: The delay of the satellite
δ_r^s	: The delay of the multipath
δt^s	: Satellite clock error
δt_r	: Receiver clock error
ϕ	: Swept phase angle at t
ϕ_0	: Unknown start phase
t	: Time
$\phi(t)$: Composite signal phase,
$\phi_r(t)$: Phase of the simulated signal,
$\phi_{GPS}(t)$: The carrier signals
N_r^s	: Integer phase ambiguity between the satellite and the receiver
$\phi_r(T)$: The phase of the simulated signal generated by the receiver
$\phi^s(T)$: Phase of the input signal from s
B_r^s	: Carrier phase bias

ABBREVIATIONS

BEIDOU	: Global Navigation Satellite System
CDMA	: Code Division Multi-Access
DOY	: Day of Year
EUREF	: European Reference Frame

LIST OF SYMBOLS AND ABBREVIATIONS (continued)

FTP	: File Transfer Protocol
GALILEO	: Global Navigation Satellite System
GLONASS	: Globalnaya Navigatsionnaya Sputnikovaya Sistema or Global Navigation Satellite System
GNSS	: Global Navigation Satellite System
GPS	: Global Positioning System
QZSS	: The Quasi-Zenith Satellite System
IGS	: International GNSS Service
IMLA	: Integrated Multipath Limiting Antenna
LAAS	: Local Area Augmentation System
LOS	: Line of sight
NASA	: National Aeronautics and Space Administration
RHCP	: Right hand circularly polarized
RINEX	: Receiver Independent Exchange Format
SNR	: Signal Noise Rate
UNAVCO	: University NAVSTAR Consortium



CHAPTER 1

INTRODUCTION AND OVERVIEW

1.1 BACKGROUND

Global Navigation Satellite Systems (GNSS) that consist of US's GPS, Russia's GLONASS, China's BeiDou, Japan's QZSS, and EU's Galileo provides three-dimensional position, velocity, and time information to an unlimited number of users anywhere near on the Earth in real-time positioning and regardless of weather conditions for marine, air and land navigation, which have been widely used in geodesy, attitude determination, engineering survey, and agricultural applications. The Russian Global Orbiting Navigation Satellite System (GLONASS) constellation has been revitalized with 24 operational satellites in orbit since 2012. On the other side, the Global Positioning System (GPS) that is owned by the United States Government whose constellation consists of 32 satellites as of February 2016 but 31 of which are in use.

It can be stated that the Global Navigation Satellite System (GNSS) is designed to serve both civilian and military applications. (Chang and Juang 2008) However, affecting the performance of GNSS suffers from random and systematic errors like ionospheric delay, tropospheric delay, ephemeris error, receiver noise and multipath. One of these is well known that multipath represents a major error source in differential GNSS positioning. Most of these errors can be removed by differential techniques. However, multipath and the receiver noise error are independent for each receiver. A number of techniques, most notably narrow correlator technology, and filtering methods, have been developed to mitigate multipath errors, while it is important to know multi-path variation characteristics (Jin et. al. 2011 and 2013).

1.2 RECENT PROGRESS AND PROBLEMS

1.2.1 Progress

The first paper that modeled and characterized multipath effects was published by Hagerman in 1973 and the fundamental relationships between code error due to multipath and the driving parameters were derived. In addition Counselman and Gourevitch were also published at the same topic in 1981. Another study of multipath published by Georgiadou and Kleusberg in 1988 that was shown which the presence of multipath can be identified by using double-differenced phase observations. Then in time, many researchers have been involved in the characterization and modeling of this propagation phenomenon. Numerous scientific papers have been published the perspective of different approaches and investigating an aspect of the problem on this topic. Thereby, the literature on multipath can appear very rich for scientists.

1.2.2 Motivation

The influence of multipath as a dominant positioning source in GNSS has been investigated from several directions with different approaches. Publications by Elosegui et al. (1995), Park et al. (2004), the initial study to evaluate the pseudo-range multipath at Differential GPS (DGPS) and Nationwide Differential GPS (NDGPS) sites by Hilla and Cline (2004) and Bilich (2006) analyzed multipath at GPS stations used for reference network and geodetic applications. These studies highlight that multipath is site-specific, with error magnitudes ranging from centimeters to meters depending on the particular environment. As just mentioned that many studies are conducted at permanent GPS stations or between two stations which are very close due to the fact that the multipath effect is closely related to the environmental influence. The technique takes advantage of the daily repetition of the GPS observations to form a multipath template (Bishop et al. 1994). Several models i.e. planar reflector models developed by Van Nee (1995), Brenner et al. (1998) and Byun et al. (2002), to sophisticated models (Lippincott et al. 1996, Axelrad et al. 1999) for varied of multipath environments have been published.

On the other hand, in some studies, the multipath effects on aircraft receivers have been characterized and modeled. For example, Braasch presented detailed models for multipath errors, including error envelopes for diverse front-end and code tracking configurations and

analyzed multipath in experimental data collected onboard a DC-3 aircraft in 1992. Another study, code multipath on a variety of commercial transport aircraft likely to utilize the Local Area Augmentation System (LAAS), ranging from Boeing 737 to 747 aircraft were characterized by Booth et al. (2000) and Murphy et al. (1996, 2004, 2005). Another study of multipath on Boeing 777 aircraft using a software GPS receiver was published by Akos et al. (2004). Even if there are a few studies on the shipboard multipath, Lachapelle et al. presented L1 C/A code multipath aboard a Canadian Coast Guard Ship. When we look at the results, we see that the ship in the stationary case is at least %90 of multipath error for more than 20 sec, but this rate falls the range of %60-75 on the moving ship. Another paper about several simulations of ship multipath was published by Ryan (2000). The simulation results confirmed that the multipath is related to the size of the ship. In other words, the icebreaker simulations sometimes yielded multipath magnitudes of tens of meters, whereas the survey launch ship errors remain under 2 meters. A lot of effort was also given on the antenna design. Brown and Gerein presented a digital beamforming antenna array which attenuated signals arriving from a direction other than the line-of-sight in 2001. The next year Thornberg et al. developed a fixed radiation integrated multipath limiting antenna (IMLA), which provides differential C/A code corrections. In both papers, the antenna patterns were designed to reduced multipath effect caused by the ground.

It should be considered that different attempts need to reduce multipath effects. Clearly, the best way to reduce the effects of multipath is to try avoiding it in the first place by sitting the receiver's antenna as low as possible and far away from potential reflectors. But that's not always feasible. The next approach is to reduce the level of the multipath signal entering the receiver by attenuating it with a suitably designed antenna i.e. ground planes, multi-beam antennas or choke ring antennas and also microwave-absorbing materials placed in an antenna's vicinity. In another way, the multipath effect can be reduced by special receiver correlator designs which aim the effect of multipath on code-phase measurements and the resulting pseudo-range observations (Langley 2011). Among these attempts, Ge et al. calculated the multipath effect using the linear combinations of GPS observations that were also used to characterize the multipath in this thesis and mitigated the multipath effect by an adaptive filter. (Ge et al. 2000) Bilich and Larson (2007), Comp and Axelrad (1998) have reduced the multipath effect by analyzing the signal-noise-rate (SNR). Besides, different multipath mitigation techniques are presented in the literature i.e. early-minus-late delay lock loop, double

delta ($\Delta\Delta$), early-late-slope, a posteriori multipath estimation, multipath estimating delay lock loop, vision correlator, etc.

GAMIT/GLOBK software was used to investigate the effect of the multipath on the position component in this thesis. There is other software in the evaluation of GPS data. This software has two types as commercial and scientific. While some of the commercial software is ASHTECH OFFICE SUITE, PINNACLE, SKI PRO, some of the scientific software is GAMIT/GLOBK, BERNESE, and GIPSY (Yıldız et. al. 2009). GAMIT/GLOBK is comprehensive GPS analysis package developed by MIT, the Harvard-Smithsonian Center for Astrophysics (CfA), Scripps Institution of Oceanography (SIO) and Australian National University for estimating station coordinates and velocities, stochastic or functional representations of post-seismic deformation, atmospheric delays, satellite orbits, and Earth orientation parameters (Herring et.al 2015). In the GAMIT evaluation, the days with the highest of MP1-RMS and MP2-RMS values were used from daily the GPS data of the processed stations. Time-series graphs of them were created. The results obtained from the GAMIT evaluation were described in detail in section 4.

1.3 MAIN CONTENT

The objective of this dissertation is to characterize the long-time variation of multipath by evaluating the amount of pseudo-range multipath with using the linear combinations for both pseudo-ranges P_1 and P_2 and carrier phase L_1 and L_2 data with eliminating the effect of receiver and satellite clocks as well as atmospheric delay from GPS and GLONASS observations. The pseudo-range multipath assessment considered in this thesis was performed using the data in Djibouti of DJIG station, Greece of DYNG station, Kenya of MAL2 station, Mayotte of MAYG station and finally, in Seychelles of SEYG station (see Figure 1) that collected GNSS data in compressed RINEX format from the global network of permanent GNSS receivers supporting the International GNSS Service (IGS) operating at a 30-second sampling rate and containing 24 hours of data in 2014, 2015 and 2016.



Figure 1.1. Processed stations.

The average daily root means square pseudo-range multipath variations (MP1-RMS and MP2-RMS) have been analyzed using TEQC software. (Estey and Meertens 1999) In this thesis, it has been also searched the other possible errors that might affect the multipath effect like seasonal changes based on natural events such as snowfall. In conclusion, the performance of GPS and GLONASS have been determined with respect to pseudo-range multipath. Contributed to the understanding of the pseudo-range multipath errors of the analysis results. This research has furthermore presented a variety of multipath mitigation techniques and analyzed the performance of different multipath mitigation techniques. So, in light of this information, this thesis will contribute to the understanding of GNSS multipath.



CHAPTER 2

MULTIPATH ESTIMATION

2.1 GNSS OBSERVATIONS EQUATIONS

GPS positioning is basically based on the principle of resection which is one of the oldest techniques in geodesy. The basic operation of the GPS receiver is to record signals from all directions and calculate pseudo-ranges using these signals. It is found by scaling the time difference (signal path time) up to the moment the signal arrives from the receiver through the satellite. This length value is mainly affected by atmospheric effects such as signal delay, signal reflection, etc. errors.

The two basic GPS observables. Which can be used for determining user position, are, in practice, simply classified as code observations and carrier phase observations. While carrier phase observations are used in high accuracy requirements and applications for scientific purposes, code observations are preferred lower accuracy applications such as navigation. (Kahveci and Yıldız 2012) In particular, the use of phase observations is inevitable for geodetic applications. To better understand GPS observables are described.

2.1.1 Code Observations

The code observations are roughly the measurements of the signal during the journey and can actually be defined as the length between the receiver and satellite antenna phase centers. This length value is expressed as a pseudo-range due to the clock offset- δ_i on both the satellite and the receiver. If it is assumed that is coincident with GPS clock and that any atmospheric influx from the satellite is accepted to be delivered to the receiver without being exposed, then the pseudo-range measured is equal to the geometric distance.

$$\rho_a^u(t) = c(t_a(t) - t_u(t)) \quad (2.1)$$

$t_a(t)$ represents the GPS time at which the signal reaches the receiver, $t_u(t)$ represents the GPS time at the exit from the satellite, c is the speed of light and t is the GPS time in Equation 2.1. However, since the above assumptions cannot be achieved in reality, it is necessary to add terms derived from clock errors to the so-called pseudo-range. When these terms are added,

$$\begin{aligned} P_a^u(t) &= c(t_a(t) + \delta_{ta}(t) - t_u(t) - \delta_{tu}(t)) \\ &= c[t_a(t) - t_u(t)] + c\delta_{ta}(t) - c\delta_{tu}(t) \end{aligned} \quad (2.2)$$

Where $c[t_a(t) - t_u(t)]$ defines the actual geometric distance between the satellite and receiver, $(t_a(t) - t_u(t))$ expresses the actual signal travel time and is briefly denoted as $\rho_a^u(t)$, $t_a^u(t)$, respectively. Thus, the actual geometric distance is obtained as $\rho_a^u(t) = c t_a^u(t)$.

$$P_a^u(t) = \rho_a^u(t) + c[\delta_{ta}(t) - \delta_{tu}(t - t_a^u(t))] \quad (2.3)$$

$\delta_{tu}(t)$ represents the difference between the satellite clock and the GPS time (satellite clock offset), $\delta_{ta}(t)$ also represents the difference between the receiver clock time and the GPS time (receiver clock offset) in Equation 2.3. In order to obtain the real observation equation, effects such as atmospheric effects (ionosphere, troposphere), instrumental corrections from satellite and receiver, signal reflection effect should be added.

The atmosphere is generally divided into two layers as ionosphere and troposphere. The ionosphere has electron density and is located in the upper layer of the atmosphere and is approximately 70-1000 kilometer above the ground surface. The troposphere is located in the lower layer of the atmosphere and extends from the earth's surface to a height of about 40 kilometers. By adding these effects, an explicit observation equation is obtained. (Leick 2004, Beutler et al. 2005a, Montenbruck et al. 2005, Beutler et al. 2007, Hofmann-Wellenhof et al. 2008, Nohutçu 2009. Swatschina 2009)

$$P_a^u(t) = \rho_a^u(t) + c[\delta_{ta}(t) - \delta_{tu}(t - t_a^u(t))] + I_a^u(t, f) + T_a^u(t) + M_a^u(t) + \varepsilon_a^u(t) \quad (2.4)$$

Where the transit terms are c speed of light (299792458 meter/sec), $\rho_a^u(t)$ geometric distance between satellite and receiver, $P_a^u(t)$ pseudo-range, $\delta_{tu}(t)$ the difference between the satellite time and the GPS time, $\delta_{ta}(t)$ the difference between the receiver clock time and the GPS time, $t_a^u(t)$ signal path time, $I_a^u(t, f)$ ionospheric effect, $T_a^u(t)$ tropospheric effect, $M_a^u(t)$ other effects, $\varepsilon_a^u(t)$, refer to thermal measurements noise and other unmeasurable effects in Equation 2.4.

- Geometric distance between the satellite and receiver Pythagorean theorem;

$$\rho_r^s = \sqrt{(x^s - x_r)^2 + (y^s - y_r)^2 + (z^s - z_r)^2} \quad (2.5)$$

For mathematical expressions for pseudo-range observations, the effects of ionosphere and troposphere, as well as hardware delays in satellite and receiver, must be considered. (Leick 2004)

$$P_r^s = \rho_r^s + \delta t_r c - \delta t^s c + I_r^s + T_r^s + \delta_r + \delta^s + \delta_r^s + \varepsilon \quad (2.6)$$

I_r^s that is in Equation 2.6, is the ionospheric delay and T_r^s is the tropospheric delay. Both are always positive. Furthermore, δ_r indicates the receiver hardware delay, δ^s indicates the delay of the satellite and δ_r^s indicates the delay of the multipath depending on the direction. ε denotes the pseudo-range measurement correction depending on the technology used.

The location (x^s, y^s, z^s) and the satellite clock error (δt^s) are known from the navigation message. Other effects (excluding noise) are determined by various models. The receiver coordinates (x_r, y_r, z_r) and the receiver clock error (δt_r) are unknowns in Equation 2.7. For the resolution of these four unknowns, four coarse edge measurements made simultaneously to four satellites are needed. Let's assume that the receiver r is observing four satellites ($s = 1, 2, 3, 4$).

$$\begin{aligned} P_r^{s1} &= \sqrt{(x^{s1} - x_r)^2 + (y^{s1} - y_r)^2 + (z^{s1} - z_r)^2} + c \delta t_r \\ P_r^{s2} &= \sqrt{(x^{s2} - x_r)^2 + (y^{s2} - y_r)^2 + (z^{s2} - z_r)^2} + c \delta t_r \\ P_r^{s3} &= \sqrt{(x^{s3} - x_r)^2 + (y^{s3} - y_r)^2 + (z^{s3} - z_r)^2} + c \delta t_r \\ P_r^{s4} &= \sqrt{(x^{s4} - x_r)^2 + (y^{s4} - y_r)^2 + (z^{s4} - z_r)^2} + c \delta t_r \end{aligned} \quad (2.7)$$

The pseudo-range observation equations are first linearized to find the position of the receiver point. Adjustment is then performed using the Least Squares Method. Accordingly, equations are not linear but are linearized using Taylor Series. (ignoring the second and higher terms)

P observation is a function of x, y, z, δt_r parameters ($P(x, y, z, \delta t_r) + \varepsilon$). Let P_0 be a calculated form of P_0 with approximate values $x_0, y_0, z_0, \delta t_{r0}$ (P_0 is required to make it linear). With Taylor Series Expansion;

$$\begin{aligned} P(x_r, y_r, z_r, \delta t_r) &\cong P(x_0, y_0, z_0, \delta t_{r0}) + (x_r - x_0) \frac{\partial P}{\partial x} + (y_r - y_0) \frac{\partial P}{\partial y} + (z_r - z_0) \frac{\partial P}{\partial z} + (\delta t_r - \delta t_{r0}) \frac{\partial P}{\partial \delta t_r} \\ &= P_0 + \frac{\partial P}{\partial x} \Delta x + \frac{\partial P}{\partial y} \Delta y + \frac{\partial P}{\partial z} \Delta z + \frac{\partial P}{\partial \delta t_r} \Delta \delta t_r \end{aligned} \quad (2.8)$$

$$\Delta P = P - P_0 \quad (2.9)$$

$$\Delta P \cong \frac{\partial P}{\partial x} \Delta x + \frac{\partial P}{\partial y} \Delta y + \frac{\partial P}{\partial z} \Delta z + \frac{\partial P}{\partial \delta t_r} \Delta \delta t_r + \varepsilon \quad (2.10)$$

Equation 2.10 can be also shown in matrix form:

$$\Delta P = \begin{bmatrix} \frac{\partial P}{\partial x} & \frac{\partial P}{\partial y} & \frac{\partial P}{\partial z} & \frac{\partial P}{\partial \delta t_r} \end{bmatrix} \begin{bmatrix} \Delta x \\ \Delta y \\ \Delta z \\ \Delta \delta t_r \end{bmatrix} + \varepsilon \quad (2.11)$$

Equation 2.11 for four satellites is:

$$\begin{bmatrix} \Delta P^{s1} \\ \Delta P^{s2} \\ \Delta P^{s3} \\ \Delta P^{s4} \end{bmatrix} = \begin{bmatrix} \frac{\partial P^{s1}}{\partial x} & \frac{\partial P^{s1}}{\partial y} & \frac{\partial P^{s1}}{\partial z} & \frac{\partial P^{s1}}{\partial \delta t_r} \\ \frac{\partial P^{s2}}{\partial x} & \frac{\partial P^{s2}}{\partial y} & \frac{\partial P^{s2}}{\partial z} & \frac{\partial P^{s2}}{\partial \delta t_r} \\ \frac{\partial P^{s3}}{\partial x} & \frac{\partial P^{s3}}{\partial y} & \frac{\partial P^{s3}}{\partial z} & \frac{\partial P^{s3}}{\partial \delta t_r} \\ \frac{\partial P^{s4}}{\partial x} & \frac{\partial P^{s4}}{\partial y} & \frac{\partial P^{s4}}{\partial z} & \frac{\partial P^{s4}}{\partial \delta t_r} \end{bmatrix} \begin{bmatrix} \Delta x \\ \Delta y \\ \Delta z \\ \Delta \delta t_r \end{bmatrix} + \begin{bmatrix} \varepsilon^{s1} \\ \varepsilon^{s2} \\ \varepsilon^{s3} \\ \varepsilon^{s4} \end{bmatrix} \quad (2.12)$$

If Equation 2.12 is written with matrix symbols, then:

$$\mathbf{b} = \mathbf{Ax} + \boldsymbol{\varepsilon} \quad (2.13)$$

Here;

\mathbf{b} : column matrix of observations,

\mathbf{x} : column matrix of unknowns,

\mathbf{A} : matrix of coefficients (including partial derivatives),

$\boldsymbol{\varepsilon}$: Noise effect matrix.

There are linear relationships between the column matrix of the observations (\mathbf{b}) and the column matrix of the unknowns (\mathbf{x}). The matrix of coefficients (\mathbf{A}) is as follows for four satellites:

$$\mathbf{A} = \begin{bmatrix} \frac{x_0 - x^{s1}}{\rho_r^{s1}} & \frac{y_0 - y^{s1}}{\rho_r^{s1}} & \frac{z_0 - z^{s1}}{\rho_r^{s1}} & c \\ \frac{x_0 - x^{s2}}{\rho_r^{s2}} & \frac{y_0 - y^{s2}}{\rho_r^{s2}} & \frac{z_0 - z^{s2}}{\rho_r^{s2}} & c \\ \frac{x_0 - x^{s3}}{\rho_r^{s3}} & \frac{y_0 - y^{s3}}{\rho_r^{s3}} & \frac{z_0 - z^{s3}}{\rho_r^{s3}} & c \\ \frac{x_0 - x^{s4}}{\rho_r^{s4}} & \frac{y_0 - y^{s4}}{\rho_r^{s4}} & \frac{z_0 - z^{s4}}{\rho_r^{s4}} & c \end{bmatrix} \quad (2.14)$$

These equations can also be edited for m number of satellites. As a result, coordinates of the observed point are found by adjustment with Least Squares Method.

$$\hat{x} = (A^T A)^{-1} A^T b \quad (2.15)$$

2.1.2 Carrier Phase Observations

Phase measurements are used in geodetic applications that require high accuracy. In phase measurement, the size of the measurement is the difference between the phase of the satellite signal and the phase of the signal produced in the receiver. (Gülal 2000)

The phase is simply the angle of rotation. The unit for GPS analysis cycles. (Taylor and Blewitt 2006).

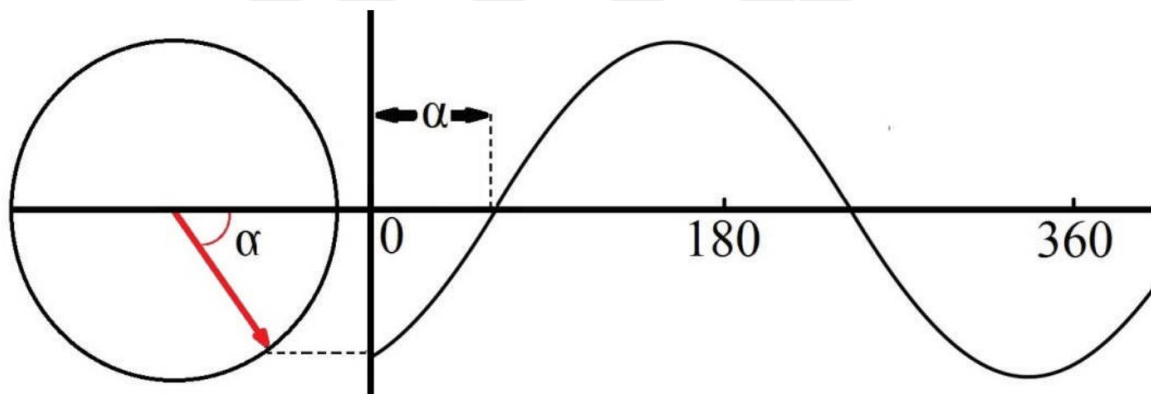


Figure 2.1. Phase Display

As shown in Fig. 2, $\phi(t)$ at any time t can be defined as the angle at which the phase sweeps during the rotation of radius, by connecting it to the center of the object for a rotating object.

$$\phi = ft + \phi_0 \quad (2.16)$$

Here;

ϕ : Swept phase angle at t ,

ϕ_0 : Unknown start phase,

f : Signal frequency,

t : Time.

Equation 2.1 shows that the phase increases linearly with time. The phase here is an ideal clock phase. Because the frequency is constant. The definition of time in everyday life is often based on rotational movement. For this reason, our time dimension can be expressed by the angle of rotation or phase (Şanlı 2000).

GPS signals are in sinusoidal form. GPS signals are called “carrier signals” (L₁ and L₂ signals). The carrier provides access to the phase-sensitive GPS time of the signal. The carrier signal transmitted from the satellite is multiplied by the simulated signal generated by the receiver and a composite signal is generated. The phase of this composite signal is equal to the difference between the phases of the carrier signal and the simulated signal.

$$\phi(t) = \phi_r(t) - \phi_{GPS}(t) \quad (2.17)$$

Here;

$\phi(t)$: Composite signal phase,

$\phi_r(t)$: Phase of the simulated signal,

$\phi_{GPS}(t)$: The carrier signal (phase of the GPS signal).

The phase difference can be measured with GPS. In this case, Equation 2.17 can also be expressed as the carrier phase difference. The carrier phase difference can be also shown with the following equation:

$$\phi(t) = \phi(t) + N_r^s \quad (2.18)$$

N_r^s that is in Equation 2.18, is the integer phase ambiguity between the satellite and the receiver. $\varphi(t)$ is also represented the residual part of the phase difference. The phase difference measured by the GPS receiver is obtained by adding N_r^s waves to the part.

The integer phase ambiguity must be a single value for all measurements made. If the signal is intercepted by the receiver for any reason, then a new integer phase ambiguity must be identified. The interruption of the GPS signal recorded by the receiver is called a “cycle slip”.

When the receiver shows the clock T, the phase observation $\phi_r^s(T)$ which is corresponding to the clock T, is modeled as follows:

$$\phi_r^s(T) = \phi_r(T) - \phi^s(T) - N_r^s \quad (2.19)$$

Here;

$\phi_r(T)$: The phase of the simulated signal generated by the receiver,

$\phi^s(T)$: Phase of the input signal from s.

It can also be written as:

$$\begin{aligned} \phi_r^s(T) &= f_0 T + \phi_{0r} - f_0 T^s - \phi_0^s - N_r^s \\ &= f_0 (T - T^s) + \phi_{0r} - \phi_0^s - N_r^s \end{aligned} \quad (2.20)$$

But in here the clock times of the signals sent and received (T and T^s) are different. The last three terms in Equation 2.20 are fixed and together they are called “carrier phase bias”.

In phase observations, the receivers must simultaneously record carrier phase measurements from all satellites. Also, all receivers must be sampled for exactly the same time values. However, since the receiver times are different, the actual measurement time varies from receiver to receiver.

Phase observations can be also expressed in the edge from. For this, Equation 2.20 is multiplied by the fundamental wavelength (λ_0).

$$\begin{aligned}
L_r^s(T) &= \lambda_0 \phi_r^s(T) \\
&= \lambda_0 f_0 (T - T^s) + \lambda_0 (\phi_{0r} - \phi_0^s - N_r^s) \\
&= c(T - T^s) + \lambda_0 (\phi_{0r} - \phi_0^s - N_r^s) \\
&= c(T - T^s) + B_r^s
\end{aligned} \tag{2.21}$$

The difference is the B_r^s carrier phase bias. This can be written as equality:

$$L_r^s(T) = \rho_r^s(t_r, t^s) + c\delta t_r - c\delta t^s + T_r^s - I_r^s + B_r^s \tag{2.22}$$

This equation also shows delays in the troposphere (T_r^s) and in the ionosphere (I_r^s). Since the phase accelerates in the ionosphere, I_r^s the minus sign.

The main differences between code and phase observation can be listed as follows (Leick 2004, Kahveci and Yıldız 2012):

- Code observations are absolute magnitudes.
- Corrections due to the ionosphere in observations are opposite signs. That is, minus for phase observations is a plus sign for code observations.
- As mentioned before, the phase measurement accuracy is higher than the code measurement accuracy.

In code observations, the code is expressed in terms of chip length, while in phase observations it is expressed as the number of wavelengths (cycles) of the carrier wave.

2.2 MULTIPATH DELAY

The multipath effect is caused by extraneous reflections from the presence of rocks, solar panels and other reflectors nearby objects such as buildings, the ground, trees and water surfaces that

GNSS signals can reach at the receiving antenna from not only the direct path, i.e. the line-of-sight (LOS) but also on various indirect paths owing to signal reflection or diffraction, which arrive with a certain delay, phase and amplitude difference relative to LOS component, called GNSS multipath effects (see Figure 2.2).

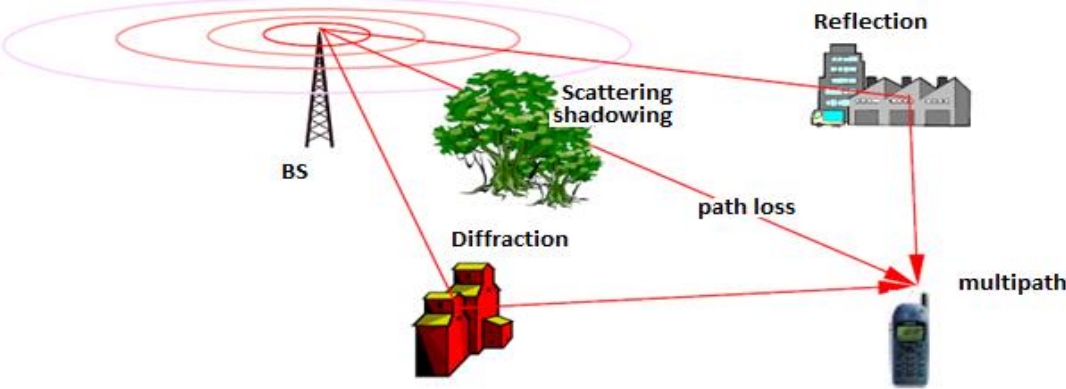


Figure 2.2. GNSS multipath model.

Hence, multipath signals travel extra distances according to the LOS signal. This relative time delay is clear that one of the defined parameters for describing the characteristics of multipath. In order to understand multipath effects, not only physical relation between the receiver and nearby objects are investigated, but also reflection characteristic is investigated as well e.g. Hannah of a Ph.D. thesis can be found typical values for the material properties for GNSS frequencies. In the case of reflection of the incident field, the reflection coefficients will indicate how much the reflected field will be attenuated and how much the polarization state of the incident field will be deformed. Besides, GNSS signals are broadcasted as linear signals, however, while signals are passing through the ionosphere, they are subjected to Faraday effect, which polarizes the signal as the amplitude increases, thus they become right-hand circularly polarized (RHCP) waves. On the other hand, they change its property after being reflected from a surface and turn into a left-hand circular polarization with a phase shift of 180° or left-hand elliptic polarization depending upon the incident angle. (Betaille et al. 2003) The basic purpose of signal processing and multipath filtering methods (receiver-based techniques) is to separate the right-hand and left-hand polarized (true and reflected) signal (Mekik and Can 2010).

According to satellites', reflectors' and receivers' states of positions, multipath signals shows three different types of scattering to become multipath errors. (Mekik et al. 2010) These different types of scatter profiles can be thought as main modes of GPS signal reflection scatter which are F mode (Forward), BA mode (Backscatter-A) and BB mode. (Backscatter-B) (Hannah 2001).

- F mode: F mode is the reflecting of signal in a forward direction from a reflector that is below the antenna altitude. F mode reflection is prominent for low elevation angle satellites. During measurement, choosing elevation angle 10 degrees higher will reduce the effect. F mode is considered as a linear reflection. (Tiryakioğlu et al. 2006) In Figure 2.3, the GPS antenna is positioned at **A** with **d** horizontal distance further away from the multipath borderline, **h** vertical distance up from the reflecting surface (ground) at an α angle to LOS and **q** distance perpendicular to the reflecting geometry.

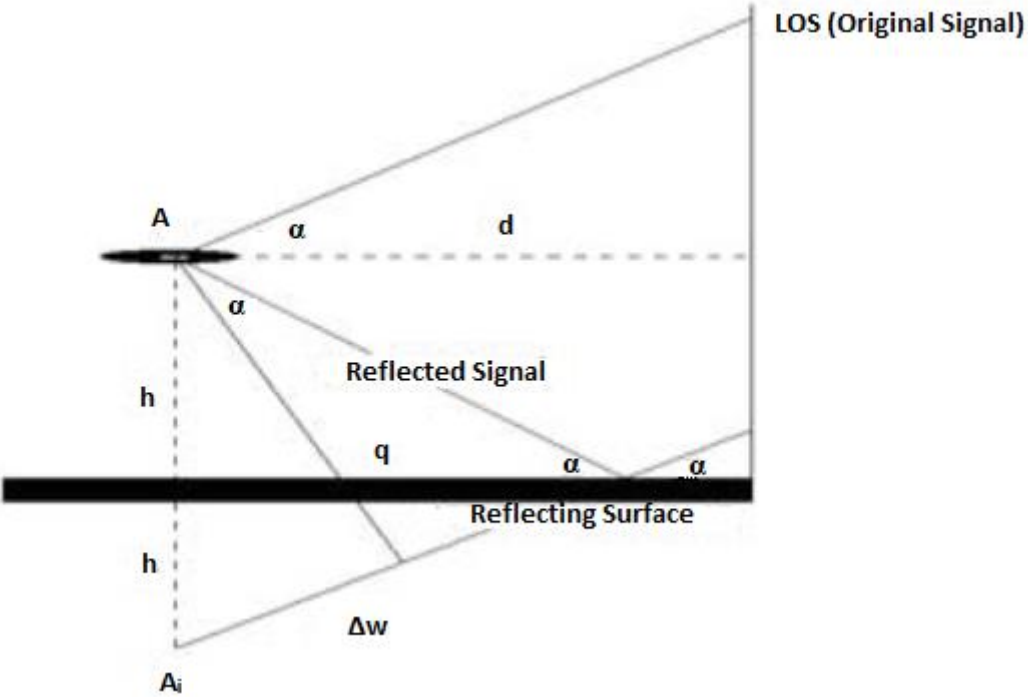


Figure 2.3. Forward scattering geometry (F-mode).

- B mode: B mode is the reflecting of signal in the backward direction from a reflector that is above the antenna altitude. To avoid this type of reflection, nested circular antenna type like choke-ring is developed. With this method, the antenna can be protected from reflected signal up to a constant angle. Over the given constant angle,

there is no solution for avoiding this reflection. This geometry is one of the main error sources for city measurements. In Figure 2.4, d is the distance between a vertical reflecting surface positioned within the left-hand borderline and the GPS antenna stationed at an arbitrary point A , α satellite elevation angle and h the antenna height.

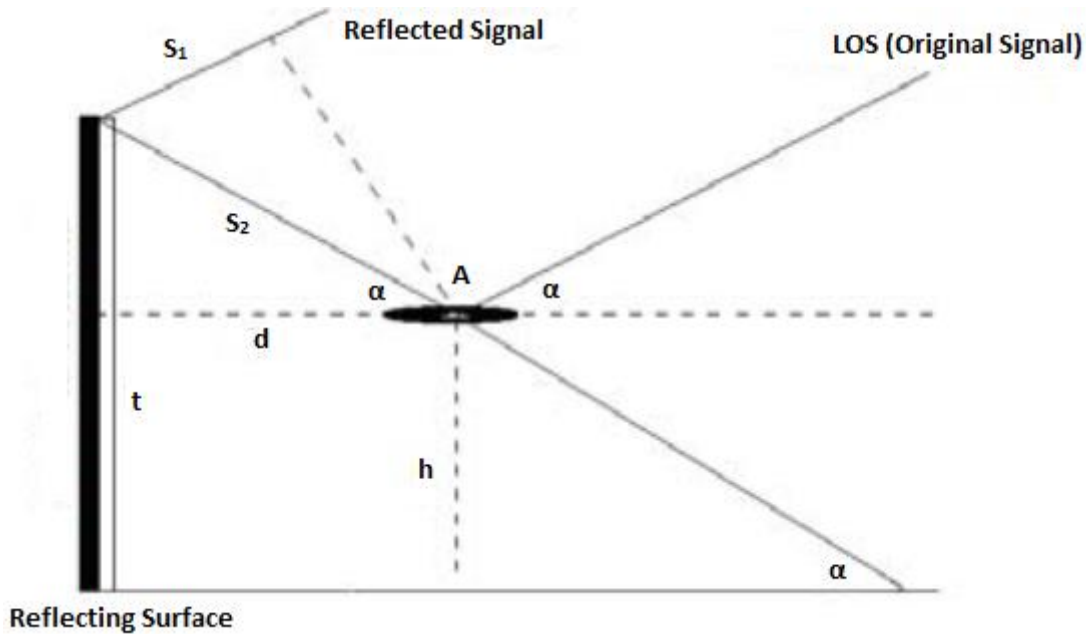


Figure 2.4. Backscattering geometry (B-mode).

- C mode: This mode can be considered as a combination of both modes discussed above. C mode is the reflecting of signal in the backward direction from a reflector below the antenna altitude. It consists of two reflections which result in RHCP wave that is detected as a GPS signal. Since it cannot be discerned from the GPS signal as it is also a RHCP wave, it is the most dangerous kind of reflection. GPS antenna positioned at point A in d distance from the reflecting surface at h height with the maximum elevation α as depicted in Figure 2.5. In addition, The S_1 and S_2 paths define the signals coming from the vertical reflecting surface while S_3 , S_4 and S_5 paths are used to describe the signals coming from first the horizontal and then the vertical surface.

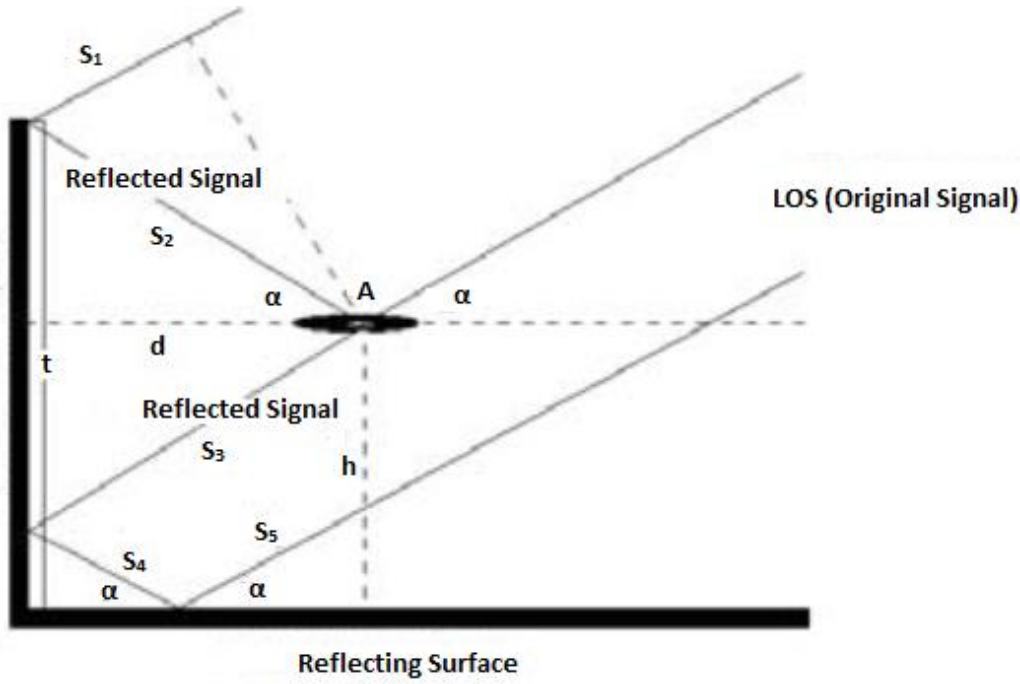


Figure 2.5. Combined Geometry (C-mode).

When the multipath phenomenon is examined that can degrade the system performance and reduce the range of measurement accuracy from centimeters to several meters. (Chang and Juang 2008) It is important that the multipath errors in the pseudo-ranges are significantly larger (up to several meters) than for carrier phases (usually, millimeter to centimeter-level). In other words, the carrier phase is less affected by multipath propagation than code ranges, because multipath is frequency-dependent. Hilla and Cline (2002) pointed out that significance of analyzing pseudo-range multipath is that the accuracy of any GPS application relies to a large extent on pseudo-range measurements. Because, the combination of direct signal and the reflected signal results in an asymmetric correlation function, resulting in an error in the computed pseudo-range to the satellite. This dissertation is also concentrated more on the effects of multipath on code measurements. Therefore, in order to identify the effective level of multipath, the linear combinations using both pseudo-range and carrier phase data used to eliminate the effects of station clocks, satellite clocks, tropospheric delay, and ionospheric delay. After the whole stages, derivation expression (Hilla and Cline 2002):

$$MP1 = P1 - \left(\frac{2}{\alpha-1} + 1\right) * L1 + \left(\frac{2}{\alpha-1}\right) * L2 = M1 + B1 - \left(1 + \frac{2}{\alpha-1}\right) * m1 + \left(\frac{2}{\alpha-1}\right) * m2 \text{ where}$$

$$B1 = - \left(1 + \frac{2}{\alpha-1}\right) * n1 * \lambda1 + \left(\frac{2}{\alpha-1}\right) * n2 * \lambda2, \alpha = \frac{f1^2}{f2^2} \quad (2.23)$$

$$MP2 = P2 - \left(\frac{2\alpha}{\alpha-1}\right)*L1 + \left(\frac{2\alpha}{\alpha-1} - 1\right)*L2 = M_2 + B_2 - \left(\frac{2\alpha}{\alpha-1}\right)*m_1 + \left(\frac{2\alpha}{\alpha-1} - 1\right)*m_2 \text{ where}$$

$$B_2 = - \left(\frac{2\alpha}{\alpha-1}\right)*n_1*\lambda_1 + \left(\frac{2\alpha}{\alpha-1} - 1\right)*n_2*\lambda_2 \quad (2.24)$$

Based on Equations 2.23 and 2.24, P1 and P2 represent the dual-frequency pseudo-range observations, L1 and L2 represent the dual-frequency carrier-phase observations and m₁ and m₂ represent the dual-frequency carrier phase multipath. The MP1 and MP2 quantities vary in time mostly due to M_i and B_i, where M_i is the pseudo-range multipath for the frequency I = 1, 2 ... and B_i is a bias related to the L1 and L2 integer carrier phase ambiguities, n₁ and n₂.

2.3 MULTIPATH ESTIMATION

Multipath is a major source of error in many GPS applications which affects both pseudo-range and carrier phase measurements and there are several methods for estimating the multipath error. The most commonly used method among them is the TEQC software that we also use in this dissertation, which is based on linear combinations of pseudo-range and carrier phase observations provided by UNAVCO, which seem to be the best option for estimating the multipath effect. This approach was proposed by Estey and Meertens (1999), Hilla and Cline (2002). The pseudo-range and carrier phase measurements on L₁ and L₂ for a satellite (k) and a receiver (i) are given by:

$$P_{L1} = R + c [\Delta t^k - \Delta t_i] + I_{L1} + T + MP_{P1} \quad (2.25)$$

$$P_{L2} = R + c [\Delta t^k - \Delta t_i] + I_{L2} + T + MP_{P2} \quad (2.26)$$

$$\Phi_{L1} = R + c [\Delta t^k - \Delta t_i] + \lambda_{L1}N_{L1} - I_{L1} + T + MP_{\Phi L1} \quad (2.27)$$

$$\Phi_{L2} = R + c [\Delta t^k - \Delta t_i] + \lambda_{L2}N_{L2} - I_{L2} + T + MP_{\Phi L2} \quad (2.28)$$

Where:

P_{L1} and P_{L2}: pseudo-range observations (in units of m),

Φ_{L1} and Φ_{L2} : corresponding carrier phase observations on L_1 and L_2 ,

R : the geometric distance between the satellite and the receiver (in m),

c : constant speed of light (in m/s),

Δt^k : satellite clock correction (in s),

Δt_i : receiver clock correction (in s),

I_{L1} and I_{L2} : ionospheric range errors (in m),

T : tropospheric range error (in m),

N_{L1} and N_{L2} : integer ambiguities (in cycles),

MP_{L1} , MP_{L2} , $MP_{\Phi L1}$, and $MP_{\Phi L2}$: pseudo-range and carrier phase multipath, respectively (including the observational noise),

$\lambda_{L1} \approx 19$ and $\lambda_{L2} \approx 24$: wavelengths of the signals on L_1 and L_2 (in cm),

$f_1 \approx 1.5754$ and $f_2 \approx 1.2276$: frequencies of signals L_1 and L_2 , respectively (in GHz).

Taking the advantage of the relationship that between the ionospheric delay for L_1 and L_2 leads to:

$$I_{L2} = \alpha \cdot I_{L1} \quad (2.29)$$

With: $\alpha = (f_1 / f_2)^2$

Substituting ϕ_{L2} equation into ϕ_{L1} equation gives:

$$\Phi_{L1} - \phi_{L2} = \lambda_1 N_{L1} - I_{L1} + MP_{\Phi L1} - \lambda_{L2} N_{L2} + I_{L2} - MP_{\Phi L2} \quad (2.30)$$

Substituting I_{L2} Equation into $\Phi_{L1} - \phi_{L2}$ equation, grouping and simplifying yields:

$$(\Phi_{L1} - \phi_{L2}) / (\alpha - 1) = I_{L1} + (\lambda_{L1}N_{L1} - \lambda_{L2}N_{L2}) / (\alpha - 1) + (MP_{\Phi_{L1}} - MP_{\Phi_{L2}}) / (\alpha - 1) \quad (2.31)$$

Combining Equation 2.31 with Φ_{L1} equation to eliminate I_{L1} term, results in:

$$\begin{aligned} \Phi_{L1} + (\Phi_{L1} - \phi_{L2}) / (\alpha - 1) &= R + c [\Delta t^S - \Delta t_R] + T + \lambda_1 N_{L1} + (\lambda_{L1}N_{L1} - \lambda_{L2}N_{L2}) / (\alpha - 1) + MP_{\Phi_{L1}} \\ + (MP_{\Phi_{L1}} - MP_{\Phi_{L2}}) / (\alpha - 1) &= R + c [\Delta t^S - \Delta t_R] + T + b_1 + m_{\phi 1} \end{aligned} \quad (2.32)$$

Equation 2.32 is a linear combination of observed L_1 and L_2 carrier phases, where the ambiguity bias term b_1 is introduced as:

$$b_1 = \lambda_1 N_{L1} + (\lambda_{L1}N_{L1} - \lambda_{L2}N_{L2}) / (\alpha - 1) \quad (2.33)$$

While the phase multipath effect is now defined by:

$$m_{\phi 1} = MP_{\Phi_{L1}} + (MP_{\Phi_{L1}} - MP_{\Phi_{L2}}) / (\alpha - 1) \quad (2.34)$$

Combining ϕ_{L1} equation, $(\Phi_{L1} - \phi_{L2}) / (\alpha - 1)$ equation and $\Phi_{L1} + (\Phi_{L1} - \phi_{L2}) / (\alpha - 1)$ equation gives:

$$P_{L1} - [1 + 2 / (\alpha - 1)] \Phi_{L1} + [2 / (\alpha - 1)] \phi_{L2} = MP_{P1} - (\lambda_{L1}N_{L1} - \lambda_{L2}N_{L2}) / (\alpha - 1) - b_1 + MP_{\Phi_{L1}} - 2m_{\phi 1} \quad (2.35)$$

The new ambiguity bias term is now defined by:

$$B_1 = -(\lambda_{L1}N_{L1} - \lambda_{L2}N_{L2}) / (\alpha - 1) - b_1 = -[1 + 2 / (\alpha - 1)] \lambda_{L1}N_{L1} + [2 / (\alpha - 1)] \lambda_{L2}N_{L2} \quad (2.36)$$

And the new phase multipath effect is introduced as:

$$M_{\phi 1} = - (MP_{\Phi_{L1}} - MP_{\Phi_{L2}}) - m_{\phi 1} = - [1 + 2 / (\alpha - 1)] MP_{\Phi_{L1}} + [2 / (\alpha - 1)] MP_{\Phi_{L2}} = MP_{\Phi_{L1}} - 2m_{\phi 1} \quad (2.37)$$

The pseudo-range multipath MP_1 is then expressed as the linear combination from $P_{L1} - [1 + 2 / (\alpha - 1)] \Phi_{L1} + [2 / (\alpha - 1)] \phi_{L2}$ equation namely:

$$MP_1 = P_{L1} - [1 + 2 / (\alpha - 1)] \Phi_{L1} + [2 / (\alpha - 1)] \phi_{L2} = MP_{P1} + B_1 + M_{\phi1} \quad (2.38)$$

Similar derivations are performed to express MP_2 as a linear combination:

$$MP_2 = P_{L2} - [2\alpha / (\alpha - 1)] \Phi_{L1} + [2\alpha / (\alpha - 1) - 1] \phi_{L2} = MP_{P2} + B_2 + M_{\phi2} \quad (2.39)$$

With MP_{P2} , B_2 and $M_{\phi2}$ are defined similarly to MP_{P1} , B_1 and $M_{\phi1}$.

As mentioned before, the multipath error in pseudo-range measurements is significantly larger than the multipath error in carrier phase measurements. Both types of GPS measurements are delicate to the effects of troposphere, ionosphere, satellite orbits, receiver position, and clocks. Therefore, all effects can be removed except for the ambiguity bias term (B_1) which is a constant, leaving one systematic error term. Random variations in the multipath equation can be diminished by calculating the average MP_{P1} values of the satellites. Based on the derived Equations 2.38 and 2.39, the daily $MP_1 - RMS$ and $MP_2 - RMS$ variations are computed by means of MP_1 and MP_2 equations.



CHAPTER 3

RESULTS AND ANALYSIS

US's Global Positioning System (GPS) and Russia's GLONASS are considered two of the main five global navigation satellite systems in this dissertation. The constellations of these systems contain MEO satellites. Both systems consist of 24 satellites. However, the orbital arrangement of them is not the same. While GPS satellites unevenly distribute in each of six orbital planes, GLONASS satellites evenly distribute in three planes. GPS of orbital planes are inclined to the equator by 55 degrees and are separated from each other by 60 degrees in longitude. In also, the satellites' orbits are circular with a radius of about 26,560 kilometers in nominal. On the other hand, GLONASS of orbital planes have a nominal inclination of 64.8 degrees and are spaced by 120 degrees in longitude. Moreover, the orbital height is about 1,060 kilometers lower than of the GPS satellites. The technology of frequency division multi-access is employed by GLONASS, while that of code division multi-access (CDMA) by GPS. In both systems, the frequency of the C/A code is 10 times lower than the P-code frequency. In general, high signal frequencies have better range-measuring accuracy than lower frequencies. Therefore, both systems use C/A code when working with less precision and P/code when working with precision mode. As seen in the table below, GLONASS values are lower than GPS values. This indicates a slightly less accurate than GLONASS. Considering the above differences, behaviors of multipath for both systems are compared.

Table 3.1. Nominal satellite signal characteristics

	GPS	GLONASS
Carrier Signals	L ₁ : 1,575.42 MHz L ₂ : 1,227.60 MHz	L ₁ : (between 1,602.0 and 1,615.5) MHz L ₂ : (between 1,246.0 and 1,256.5) MHz
Codes	different for each satellite C/A code on L ₁ P-code on L ₁ and L ₂	same for all satellites C/A code on L ₁ P-code on L ₁ and L ₂
Code frequency	C/A code: 1.023 MHz P-code: 10.23 MHz	C/A code: 0.511 MHz P-code: 5.11 MHz
Clock data	clock offset, frequency offset, frequency rate	clock and frequency offset
Orbital data	modified Keplerian orbital elements every hour	satellite position, velocity, and acceleration every half hour

3.1 MULTIPATH TIME SERIES

Multipath effects on GPS and GLONASS satellite systems were investigated by using the linear combinations of the pseudo-ranges and carrier-phase observations. Results show large variations in different years based on the multipath estimations. These multipath estimates as MP1 and MP2 were computed with TEQC from GPS and GLONASS observations at 5 stations. The multipath time series for each station are shown in Figure 3.1. In all graphs presented, horizontal axis years, multipath values in vertical axis meter unit, dark line GPS-MP1 values, red line GLONASS-MP1 values, black line GPS-MP2 values, turquoise line GLONASS-MP2 values. These time-series graphs of the stations will be examined in the following section.

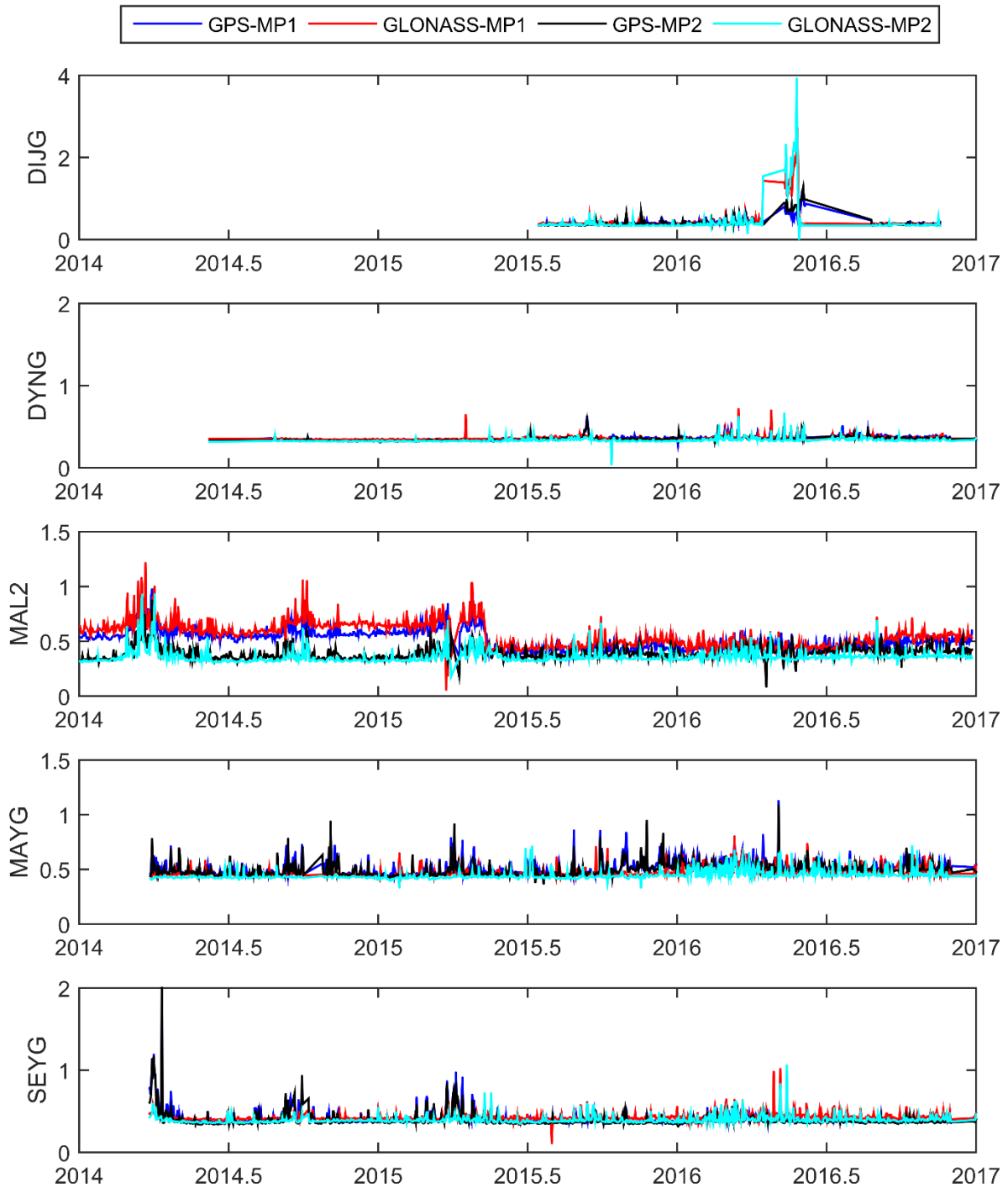


Figure 3.1. Multipath time-series

The first DJIG station was joined the IGS network on July 9, 2015. For this reason, there is no data for this station before. Also, the antenna of the DJIG station was mounted on a 0.8-meter concrete pillar embedded on the ground. (see Figure 3.3) In June 2015, the receiver with the version 4.85 was removed and the receiver with the version 5.01 was installed on the same day. The elevation cut-off angle was modified from 3° to 0° on October 29th. As the tracking

threshold of the receiver, ideally 3° or less, is determined according to IGS site guidelines, the elevation angle is modified in certain times, as in this station. On April 25, 2016, no signal was received from the station due to network failure. Also, the receiver of the station was upgraded from version 5.01 to version 5.10. The firmware version of the receiver was upgraded to 5.14 on September 5, 2016. The negative effects of this change have been shown in the red area in Figure 3.2. The station is unavailable on September 24th and on November 21st to 24th, due to some problems. On December 19th, the firmware version of the receiver was upgraded to 5.15. In addition, the negative effects of this change have been shown in the red area in Figure 3.2.

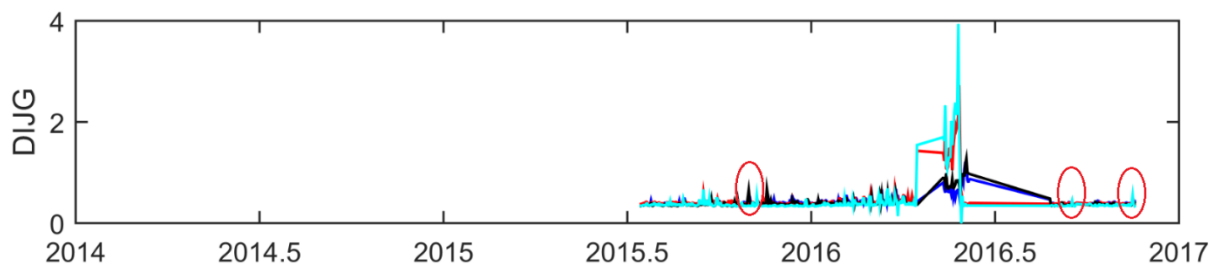


Figure 3.2. The negative effects of the multipath on the multipath time-series of DJIG station.

The receiver environment is a rocky area, the elevation cut-off angle is reduced from 3° to 0° and these factors also lead to deterioration in multipath values as shown in Figure 3.3. It is thought that DJIG station has F-Mode multipath geometry depending on the environment in which the antenna was installed.



Figure 3.3. DJIG station (IGS) with Dorne Margolin and choke rings.

Table 3.2. The changes made on DJIG station at IGS Network Site Page.

Email	Date	Sender	Subject
006017	2016/12/19	Operation Regina	DJIG : firmware upgrade
005975	2016/11/24	Bonnes Gregory (T	DJIG : Unavailable
005899	2016/09/05	Operation Regina	DJIG : firmware upgrade
005892	2016/08/25	Operation Regina	DJIG : Antenna change
005736	2016/04/25	Bonnes Gregory (T	DJIG : network issue and tracking losses
005482	2015/10/29	Lawrence Thierry	DJIG : Elevation cut-off change

As a result, the RMS-MP2 value of GLONASS is the most affected, while the RMS-MP1 of both systems have less affected as shown in Figure 3.1. However, the RMS-MP1 value of GLONASS is slightly higher than the RMS-MP1 value of GPS as shown in Figure 3.1.

The second DYNG station was installed on May 12, 2011, which is the only EUREF station, while other selected stations are from IGS Network. The antenna was mounted on a 2-meter steel block (see Figure 3.6) and used a Dorne Margolin with choke rings. On June 5, 2014, the firmware version of the receiver was upgraded from 4.70 to 4.85 and wrong antenna serial numbers were corrected. Due to a tracking problem (possible antenna failure), some observations of L₂ and L₅ at the DYNG station have been lost since on 19 August 2015. On September 25, 2015, a new antenna with the same antenna type was installed due to the loss of L₂. On October 23rd, the cut-off elevation angle of some stations, such as AREG, ASCG, CHPG, CPVG including DYNG, has been modified from 3° to 0°. Due to the file transfer protocol (FTP) in a loop on November 17th, the data were not provided during the day of the year (doy) 317 and doy 320. These are the possible causes of fluctuations. On June 8, 2016, the DYNG station is unavailable due to unknown reasons. Therefore, data cannot be provided on that day. This caused slight fluctuations in the multipath time-series, as shown in Figure 3.4.

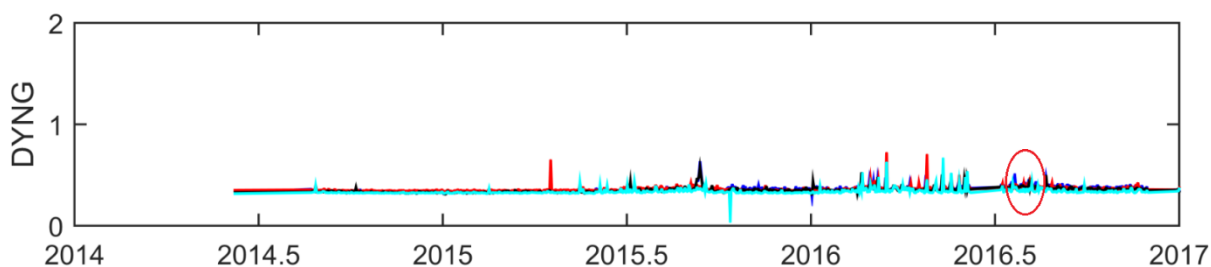


Figure 3.4. Fluctuations in the multipath time-series of DYNG station.

However, it has been available since on 5 July 2016 and the receiver has been changed for a new receiver updated with version 5.14. On December 14th, the firmware version of the receiver was upgraded from 5.14 to 5.15. The presence of a potential source in the south-west of the antenna could have caused multipath effects as shown in Figure 3.5. It is thought that DYNG station has BA-Mode multipath geometry depending on the environment in which the antenna was installed.

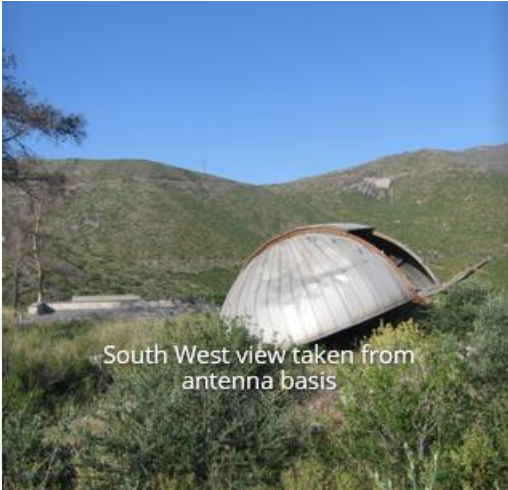


Figure 3.5. The southwest view of the receiver of DYNG station.

Compared to other stations, the DYNG station has very small multipath as shown in Table 3.3.

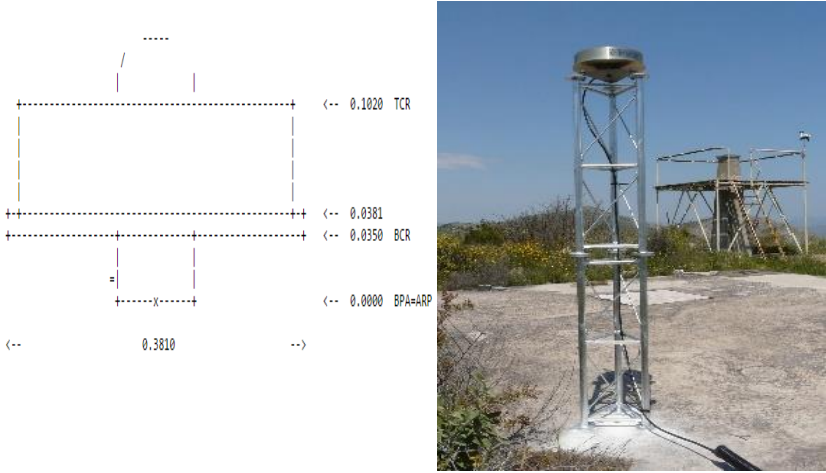


Figure 3.6. DYNG (EUREF) station with Dorne Margolin and choke rings antenna.

Table 3.3. RMS Table.

YEAR	RMS	DJIG	DYNG	MAL2	MAYG	SEYG
2014	GPS-MP1		0.01	0.08	0.05	0.14
	GPS-MP2		0.01	0.21	0.05	0.14
	GLONASS-MP1		0.004	0.09	0.02	0.02
	GLONASS-MP2		0.004	0.08	0.02	0.03
2015	GPS-MP1	0.03	0.03	0.10	0.07	0.08
	GPS-MP2	0.03	0.02	0.05	0.07	0.07
	GLONASS-MP1	0.02	0.02	0.12	0.04	0.04
	GLONASS-MP2	0.03	0.02	0.05	0.03	0.04
2016	GPS-MP1	0.10	0.02	0.05	0.06	0.05
	GPS-MP2	0.13	0.03	0.05	0.06	0.05
	GLONASS-MP1	0.27	0.04	0.06	0.06	0.07
	GLONASS-MP2	0.35	0.04	0.04	0.06	0.06

The third station, MAL2, was installed on July 1, 2008. The antenna was mounted on a 1-meter concrete pillar monument. (see Figure 15) The antenna used a Dorne Margolin with 3D choke rings. It is obvious that the MAL2 station is the most affected station by multipath as shown in Figure 3.7.

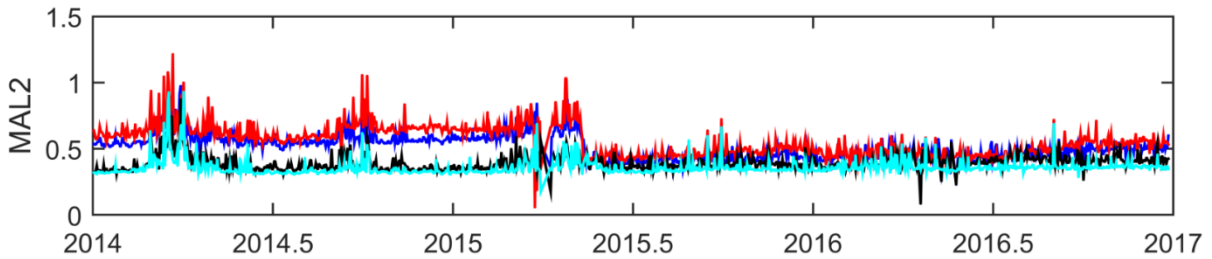


Figure 3.7. The multipath time-series of MAL2 station.

Since the type of receiver and antenna at this station has not changed until October 2016, the diversity of these results can be attributed to any kind of enhancement of the hardware. However, on October 18, 2016, the firmware version of the receiver was upgraded from 2.9.0 to 2.9.5. This change is shown in Figure 3.8 in the red box, which has a detrimental effect on multipath values.

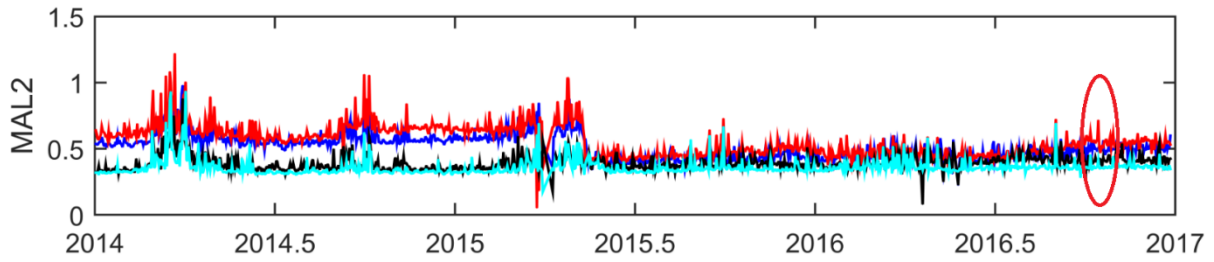


Figure 3.8. The negative effects of the multipath on the multipath time-series of MAL2 station.

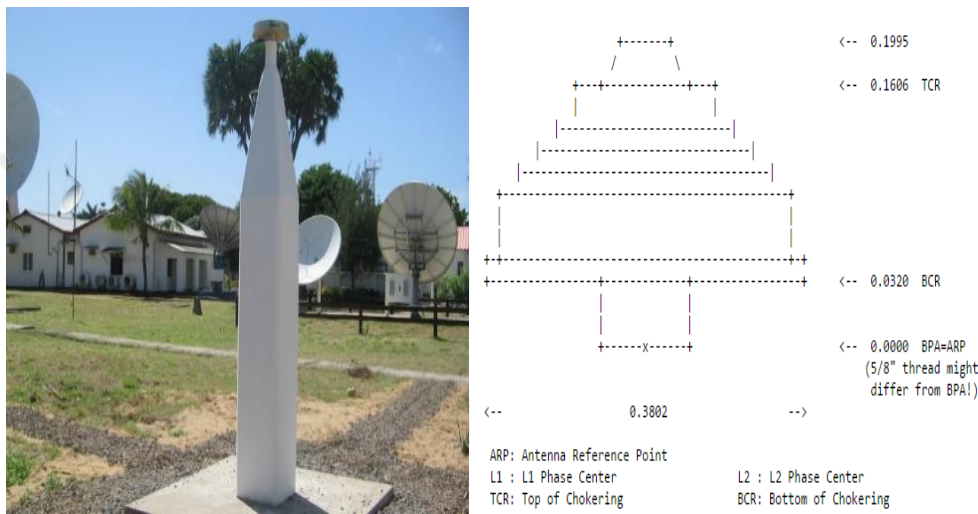


Figure 3.9. MAL2 (IGS) station with Dorne Margolin and 3D choke ring antenna.

As a result, when both systems are compared, the value of GPS-MP2 is the most affected by the multipath error as shown in Table 3.3. It is thought that MAL2 station has F-mode and BA-Mode multipath geometry depending on the environment in which the antenna was installed.

The fourth station, MAYG, was installed on November 21, 2013. The antenna of this station was mounted on a concrete block on a 3-meter steel mast and used a Dorne Margolin with choke ring antenna. (see Figure 3.11) The first version 4.81 of the TRIMBLE NETR9 receiver was used until June 11, 2014, and the firmware version of the receiver was upgraded to 4.85 on that same day. After that date, the firmware version of the receiver was upgraded twice. First, on August 9, 2016, the firmware version of the receiver was upgraded from 5.01 to 5.14. Second, on December 16, 2016, the firmware version of the receiver was upgraded from 5.14 to 5.15. The negative effect of these changes on the multipath time-series graph was shown in Figure 3.10 in the red box.

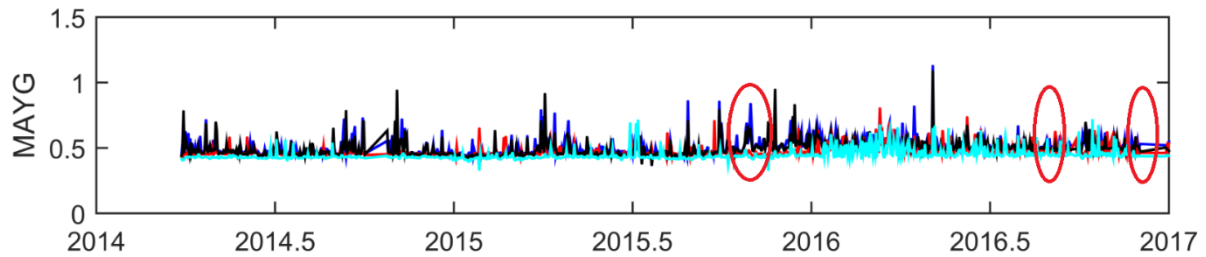


Figure 3.10. The negative effects of the multipath on the multipath time-series of MAYG station.

Furthermore, this station was not available due to the internet outage on November 9, 2015, 12 January, 17 May and 25 August 2016. Compared to the two systems, the multipath in GPS at the MAYG station are more severe than those of GLONASS. However, in 2016, the RMS values of both systems were equally affected by the multipath error as shown in Table 3.3. Except for 2016, the MP1-RMS values of the GPS are approximately 2 times as great as that of GLONASS as shown in Table 3.3. The result of multipath variations may reflect the sea-level change. (Jin et al. 2016) It is thought that MAYG station has F-mode multipath geometry depending on the environment in which the antenna was installed.

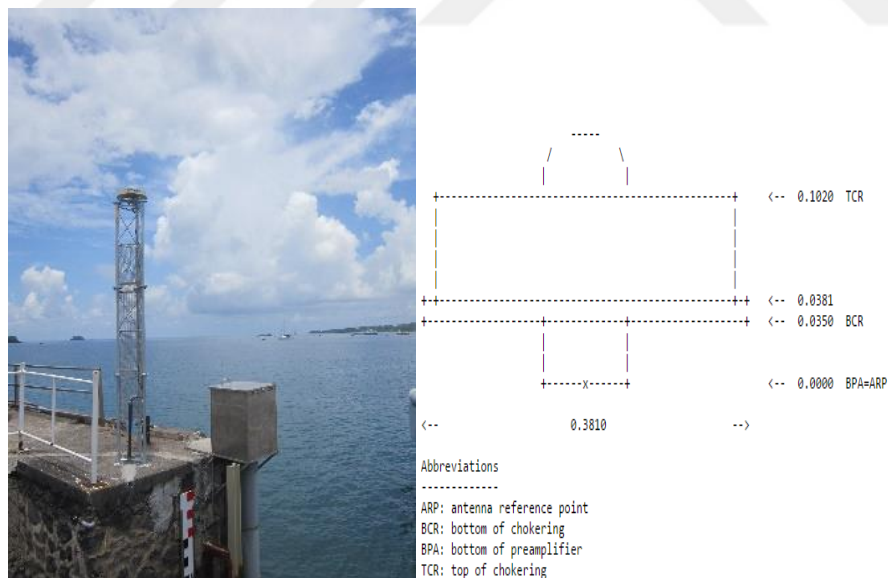


Figure 3.11. MAYG (IGS) station with Dorne Margolin and choke rings.

The last station named SEYG was installed on June 20, 2012. The antenna of this station was mounted on a 1.5 meters high concrete pillar monument with a 40 cm steel antenna. It used a Dorne Margolin with choke ring antenna. On March 6, 2014, this station was joined the IGS

Network. On June 16, 2014, TRIMBLE NETR9 receiver was upgraded to version 4.85 and used until June 16, 2015. Then, the firmware versions of the receiver were updated a few times in different years, which resulted in unusual behaviors in the multipath estimates of the station as shown in Figure 3.12 in the red box.

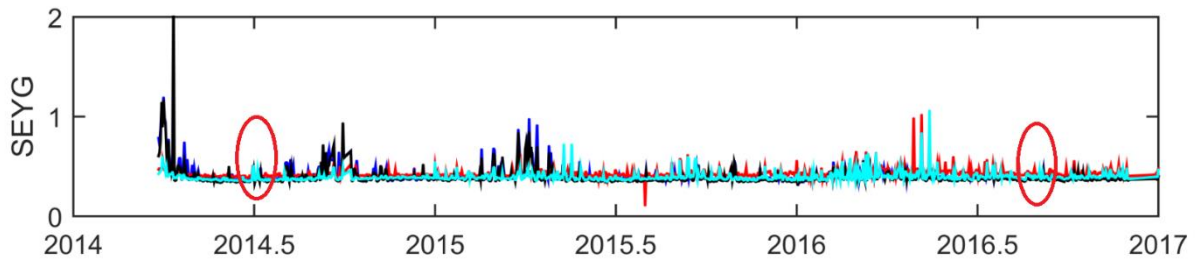


Figure 3.12. The negative effects of the multipath on the multipath time-series of SEYG station.

While the values of GPS are the most affected by the multipath errors in 2014 and 2015 years, the values of GLONASS are the most affected by the multipath errors in 2016 as shown in Table 3.3. However, there is no clear connection since this station has no information about the antenna environment. That's why it is not known which the multipath geometry this station has.

The antenna surrounding environment that affects GNSS multipath, is the main factor for multipath variations. The existence of these factors exhibits abnormal behaviors in the multipath time-series, which can be used to estimate surface environment changes in contrast. (Jin et al. 2011).

3.2. STATISTIC ANALYSIS

In this study, long-term (2014-2016) daily the root mean square (RMS) values of MP1 and MP2 belonging to 5 stations were used. They were examined to determine the changes between the two systems.

Sample trend analysis belonging to DJIG station (see Table 3.4) presents the difference between these two satellite systems visibly. The calculated RMS values for GPS and GLONASS indicate statistically significant trends. According to these values, the multipath amplitude of GPS is low and also it shows that the multipath is very weak than the multipath of GLONASS.

Table 3.4. Sample trend analysis of DJIG station.

			Trend (m)	m	A_Phase (°)	m	A_Amplitude (m)	m
	GPS	MP1	0.0318	0.0113	-31.8527	0.0486	0.1098	0.007
DJIG		MP2	0.0363	0.0126	-38.7562	0.0451	0.1566	0.0079
	GLONASS	MP1	0.0763	0.0277	-43.5057	0.0542	0.3372	0.0187
		MP2	0.0982	0.0373	-45.0943	0.0617	0.4104	0.0253

These average RMS values show which station is more or less affected by the multipath (see Table 3.5) In the direction of these values, only 10° the elevation cut-off angle has been analyzed. When compared with other stations, the DJIG station is the most affected by the MP1 and MP2 values of the GPS as shown in Table 3.5. Besides, the station that is also least affected by the multipath errors, is the DYNG station. According to GLONASS data, while the most affected station is DJIG, the least affected station is DYNG.

Table 3.5. The RMS-MP1 and RMS-MP2 values in meters.

		DJIG	DYNG	MAL2	MAYG	SEYG
GPS	MP1	0.110718	0.029702	0.09312	0.067118	0.104605
	MP2	0.138824	0.026624	0.05946	0.063562	0.099974
GLONASS	MP1	0.278886	0.03009	0.11518	0.046258	0.050398
	MP2	0.357397	0.030661	0.05964	0.043687	0.04934

Figure 3.13 describes the 3-year daily RMS values in meters.

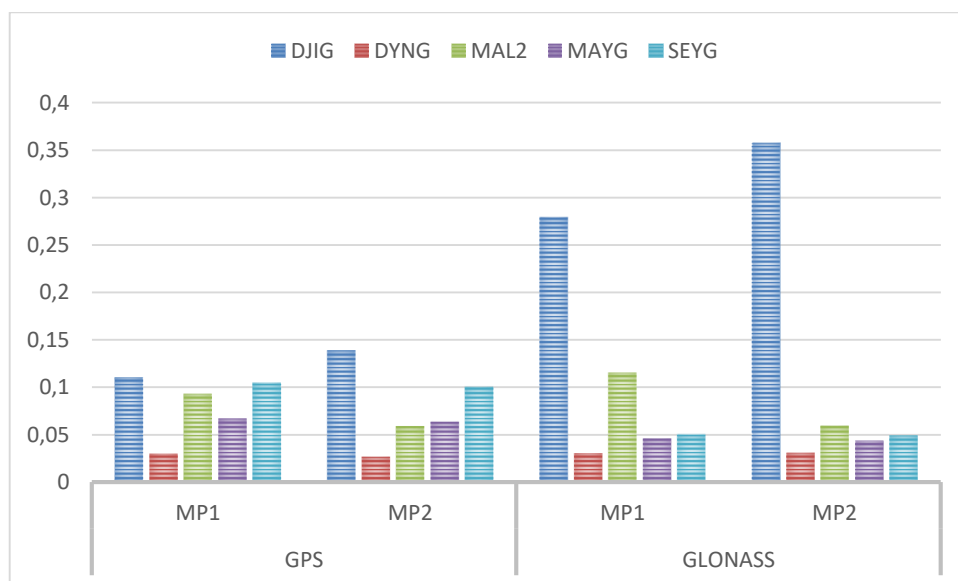


Figure 3.13. RMS-MP1 and RMS-MP2 values of all stations in both systems.

The RMS-MP1 and the RMS-MP2 statistics were made for both each station and two satellite systems and also the results which indicate that the RMS values of the stations, are shown in Figure 3.13. When compared stations each other, the results indicate that the RMS-MP1 is the largest value belonging to SEYG station on both systems. In addition, the histogram of this station has a right-skewed distribution. The histogram of DYNG station is also has a right-skewed distribution, but it has the lowest RMS value. When compared both satellite systems, the number of values that accumulate in the RMS values of the stations is slightly higher in GLONASS.

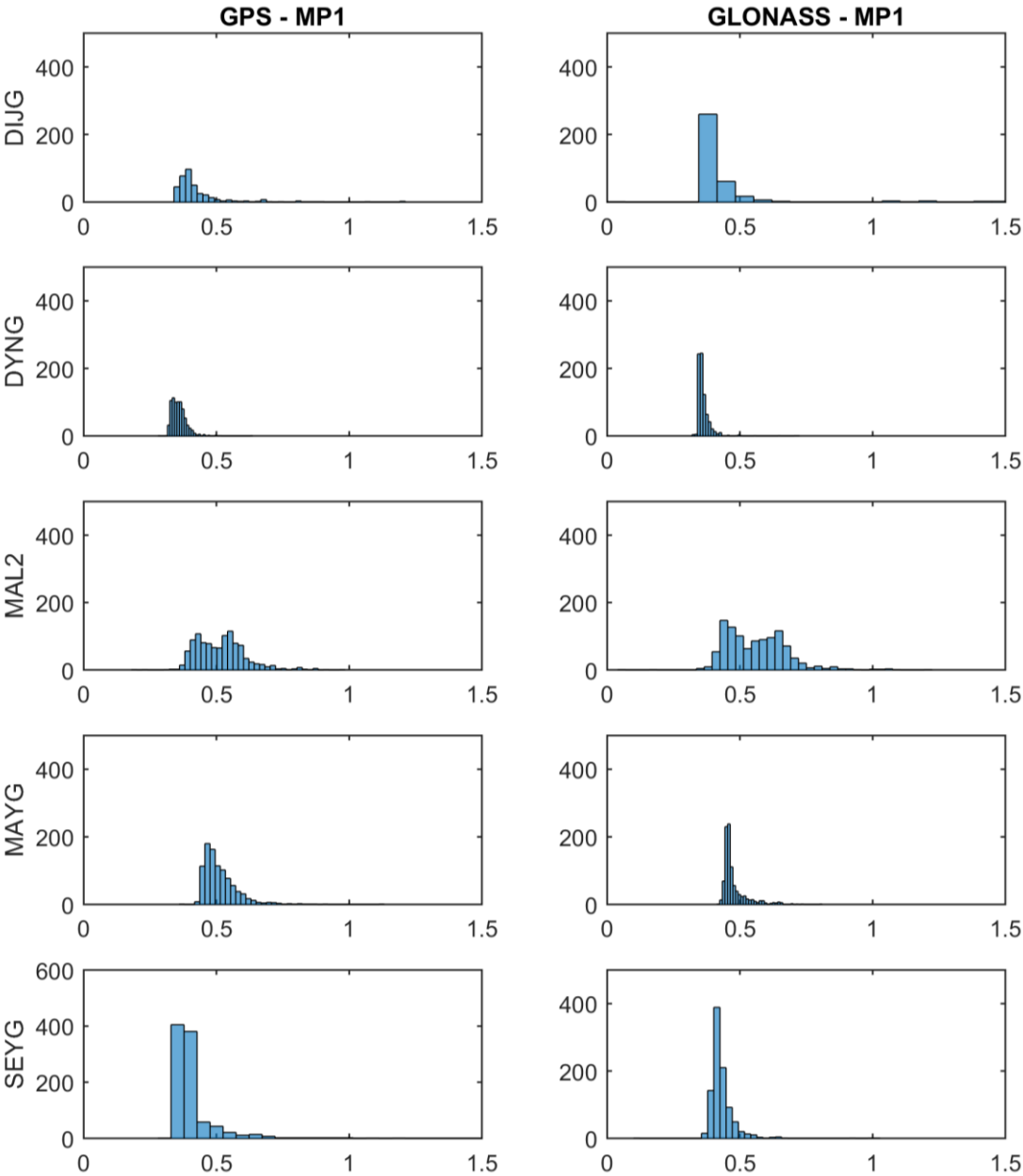


Figure 3.14. The RMS-MP1 statistics for all stations.

The acquired the RMS-MP2 values on both systems for all stations have been shown in Figure 3.15 as in the figure of the acquired the RMS-MP1 values. (see Figure 3.14) Obviously, The RMS-MP2 value of the GPS at the MAYG station is 0.06 m and also the most affected one is this station. At the same time, in GLONASS, the most affected station is MAL2 and its value is 0.07 m. On the other hand, the least affected station on both systems is the DYNG station and its value is below the decimeter.

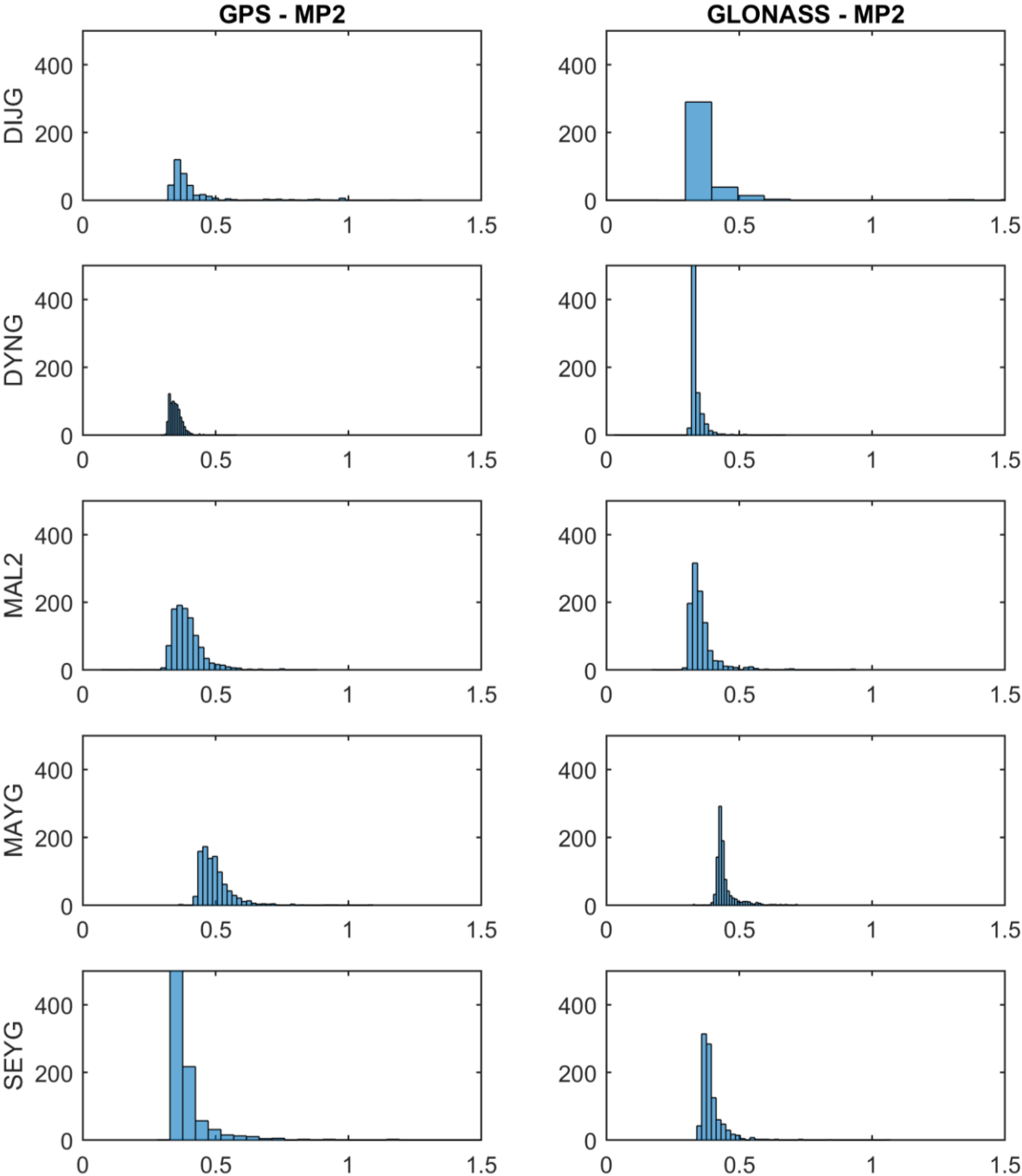


Figure 3.15. The RMS-MP2 statistics for all stations.



CHAPTER 4

POSITIONAL CHANGES

In the previous section, multipath values were examined especially in selected stations. MP1-RMS and MP2-RMS values of 0.34 to 2.22 meters were determined in this section and the effects of these values on the position component were investigated. In this context, a geodetic network was formed. This geodetic network is like the picture given in Figure 4.1.

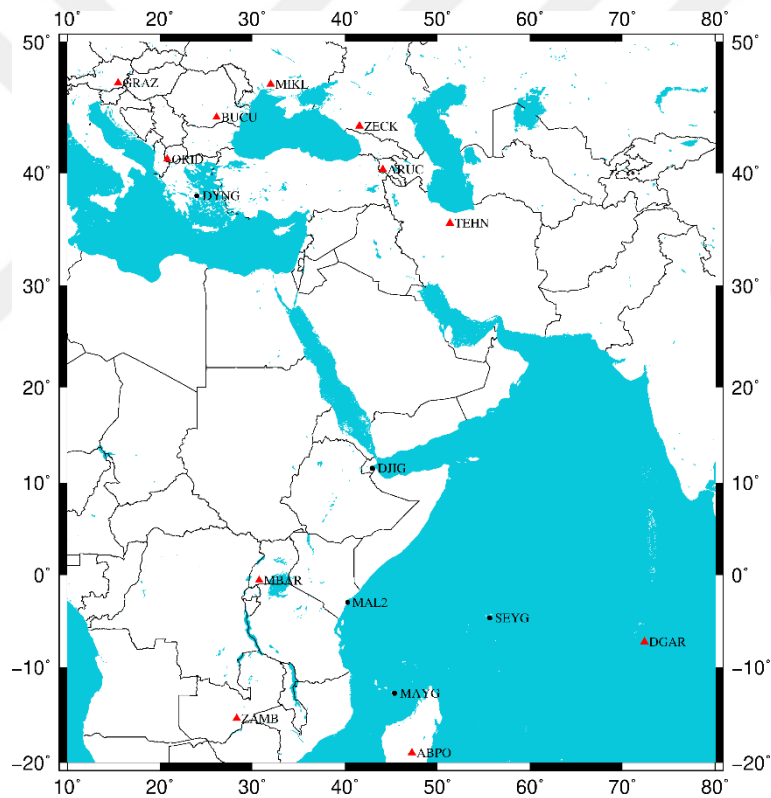


Figure 4.1. Formed geodetic network.

While the red dots show the datum points, the black dots indicate the object points in Figure 4.1. Selected datum points; DGAR in the United Kingdom on Australian tectonic plate, ABPO in Madagascar, ZAMB in Zambia and MBAR in Uganda on the African tectonic plate, also those in the Eurasian tectonic plate are ORID in Macedonia, GRAZ in Austria, BUCU in Romania, MIKL in Ukraine, ZECK in Russian Federation, ARUC in Armenia and finally

TEHN in the Islamic Republic of Iran. These IGS stations including the stations in the geodetic network are included in the analysis to investigate the effect of the multipath error on the position component. In this context, GPS data were evaluated by GAMIT (GPS Analysis Massachusetts Institute of Technology) / GLOBK (GLOBAl Kalman) software developed by MIT. The tables folder is firstly created. This contains some information about the stations (luntab, soltab files), moon and sun ephemeris information (antenna and receiver type, antenna height, initial coordinates) that will be used to evaluate data of GAMIT software. These parameters and their contents are shown in Table 4.1.

Table 4.1. Tables folder input data.

INPUT NAME	INPUT CONTENT
gdetic.dat	Geodetic datum parameters
tform.dat	Coordinate transformation parameters
antmod.dat	Ground/SV antenna phase center models
rcvant.dat	IGS receiver/antenna codes
svnav.dat	Satellite block #s, PRN #s, masses
leap.sec	GPST – UTC
luntab.	Lunar ephemeris table
nutabl.	Nutation tables (IERS/IGS standards)
soltab.	Solar ephemeris table
pole	IERS bulletin B values
Ut1	IERS bulletin UT1
itrf05.apr	Coordinate values

“Station.info, process.defaults, sites.defaults” files in the Tables folder need to be edited according to the project. Station.info file is the information file of the receiver and antenna type and antenna height of IGS stations and stations used in the project. Information about IGS stations is included in the program and only the information of the stations used in the project must be entered. Sites.defaults file contains IGS stations which will be used for data analysis, repeatability analysis, and stabilization, and the stations included in the project. In addition, it is determined that where and how the data belonging to them will be obtained. The process defaults which is the other important file in the tables folder are arranged to determine the instructions related to the workspace, internal and external data sources, orbit files, start time,

sampling interval and to archive the results. Then, it is prepared for the sestbl. file which contains the commands including all the control stages of GAMIT software. This file is organized to determine the type of analysis and possible measurement errors, satellite restrictions. Briefly, the file described as evaluation strategies provides criteria for the integer ambiguity resolution and to be defined atmospheric, orbit, model and data cleaning parameters. Solution strategies which are selected for project work and entered to the sestbl. file is given in Table 4.2.

Table 4.2. GAMIT evaluation strategy.

Parameters	Preferred Options
Solution Strategy	Baseline
Elevation Angle	10 degrees
Orbit	Final Product (IGSF)
Antenna Model	Elevation (ELEV)
Ambiguity Solution	Iono-free
Interval Zenith	2 hours
Dry and Wet Mapping Function	Vienna Mapping Function (VMF1)
Loading	63 (All)
High Order Ionosphere	Neglected

The other control file that provides models and restrictions for analysis, is sittbl. file. This file is arranged to determine the possible coordinate constraints in the workspace and optionally, the model of time and atmospheric errors. After the completion of these processes, the evaluation process is started by running the sh_gamit command to evaluate with GAMIT software. GAMIT.fatal file occurs in the day files if any errors occur during evaluation. The occurrence of this situation indicates that the solution belonging to that day has not been completed and the reason for the error has been written in the file. After passing this step, necessary checks are performed. After these checks, the next step is to obtain time series of stations in the project area. The sh_glred command is used to generate H-files and daily repeatability time series from GAMIT solution to the GLOBK solution. After GLOBK evaluation, it is possible to comment on repetitive measurements by analyzing the graphs obtained from the daily repetitions.

4.1. RESULTS

In this study, 11 IGS stations which have good performance and stability, were included in the analysis as previously mentioned including the stations in the geodetic network. The stations within this geodetic network are a high possibility of being affected by the multipath error. This high possibility of being affected by the multipath error may be related to the fact that these stations were installed on the tectonic plate. Figure 4.2 shows which tectonic plate the selected stations were installed on.

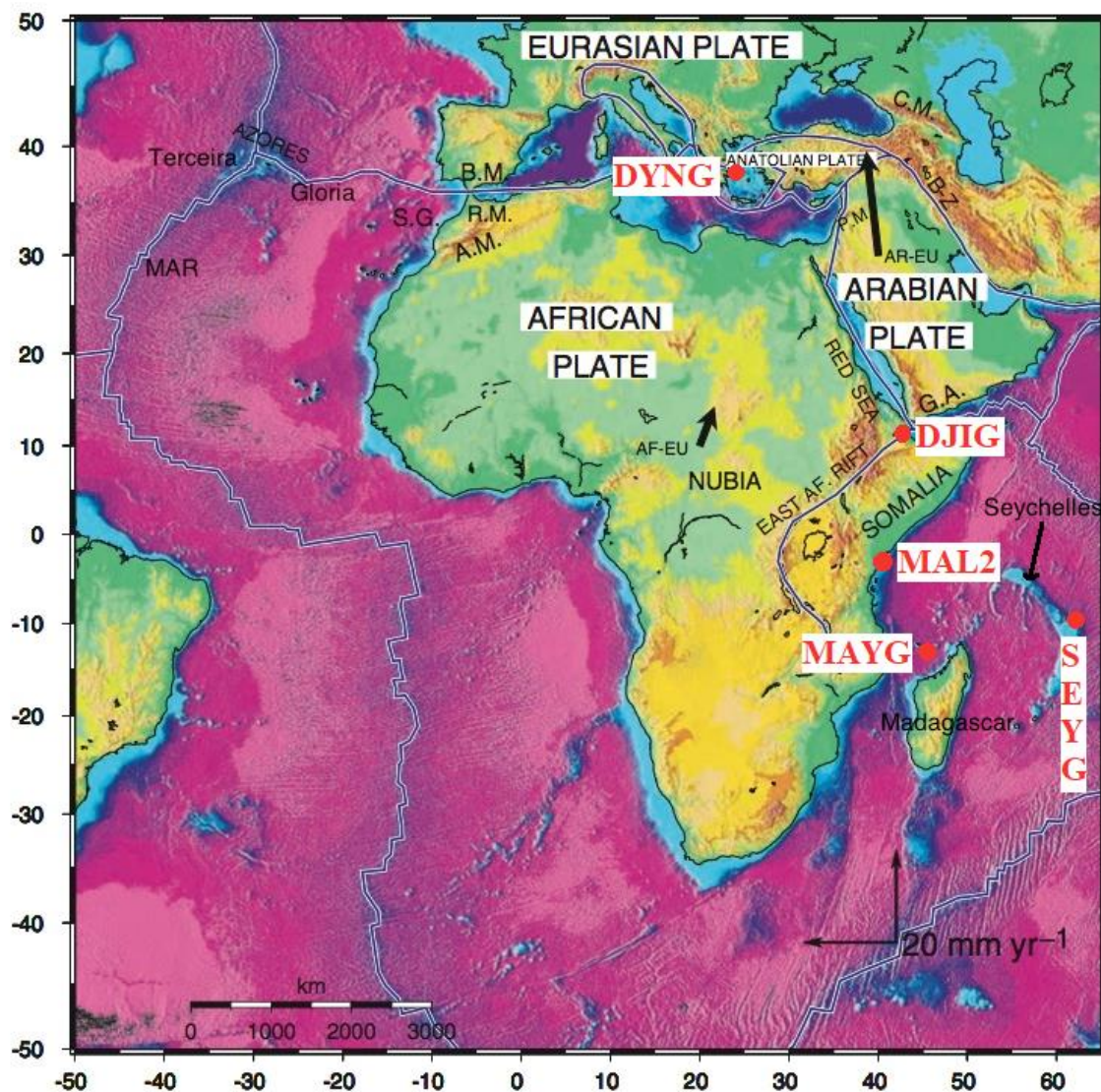


Figure 4.2. Tectonic plates of the selected stations.

During the process of the evaluation, days that are the highest MP1-RMS and MP2-RMS values belonging to the stations have been processed onto the time-series graphs. As a result of these

evaluations, the time-series graphs including the effects of the multipath errors on the position component were obtained by examining the north, east and up repeatability results in GPS of the selected stations by means of GAMIT software. The time-series obtained in this study have been shown in the following graphs, respectively. While the horizontal axis shows years, the vertical axis indicates weighted root mean square in the millimeter in the presented all graphs. In the presented all graphs, the repeatability values in the east component are shown in black, the repeatability values in the north component are shown in pink and also the repeatability values in the up component are shown in blue. Moreover, the gray color above the values represents the residual values of the station.

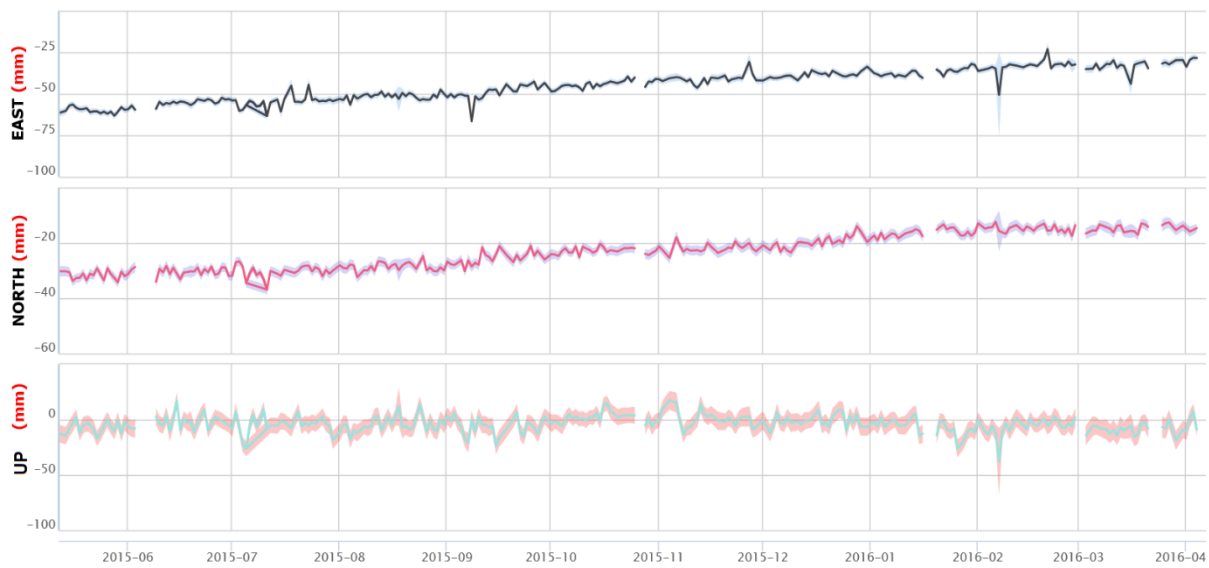


Figure 4.3. Multipath time-series of the east, north and up components belonging to DJIG station

The east, north and up components specified in Figure 4.3 belong to the DJIG station. GAMIT valuation was made between 25 July 2015 and 6 June 2016. Since the multipath values of these days are the highest (0.43 m - 1.27 m), the position changes were analyzed between these dates. Moreover, this station located on the Somalia tectonic plate was chosen because of the high multipath error.

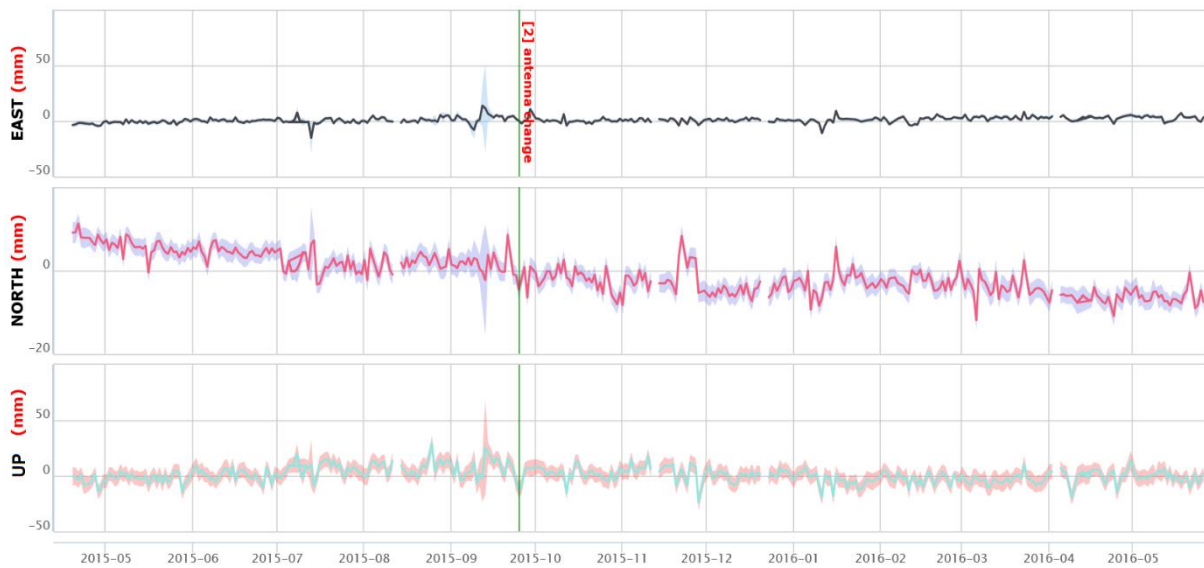


Figure 4.4. Multipath time-series of the east, north and up components belonging to DYNG station.

The east, north and up components specified in Figure 4.4 belong to the DYNG station. GAMIT valuation was made between 23 August 2014 and 6 September 2016. Since the multipath values of these days are the highest (0.33 m – 0.64 m), the position changes were analyzed between these dates. Moreover, this station located on the Eurasian tectonic plate was chosen because of the high multipath error.

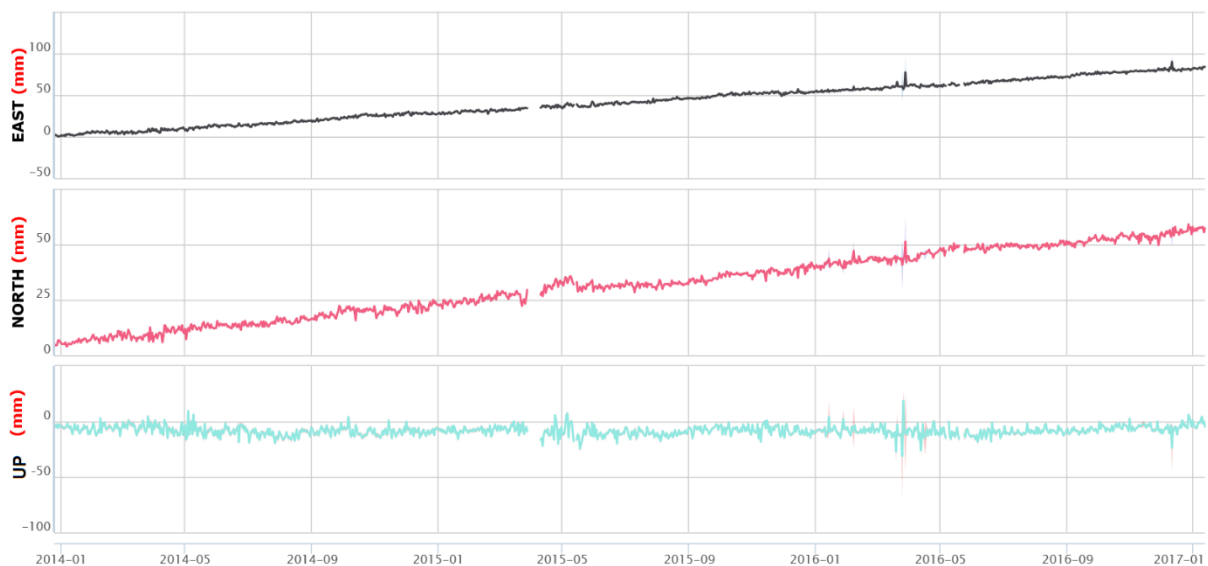


Figure 4.5. Multipath time-series of the east, north and up components belonging to MAL2 station.

The east, north and up components specified in Figure 4.5 belong to the MAL2 station. GAMIT valuation was made between 28 February 2014 and 29 December 2016. Since the multipath values of these days are the highest (0.47 m – 0.98 m), the position changes were analyzed between these dates. Moreover, this station located on the African tectonic plate was chosen because of the high multipath error.



Figure 4.6. Multipath time-series of east, north and up components in 2015 and 2016 belonging to MAYG station.

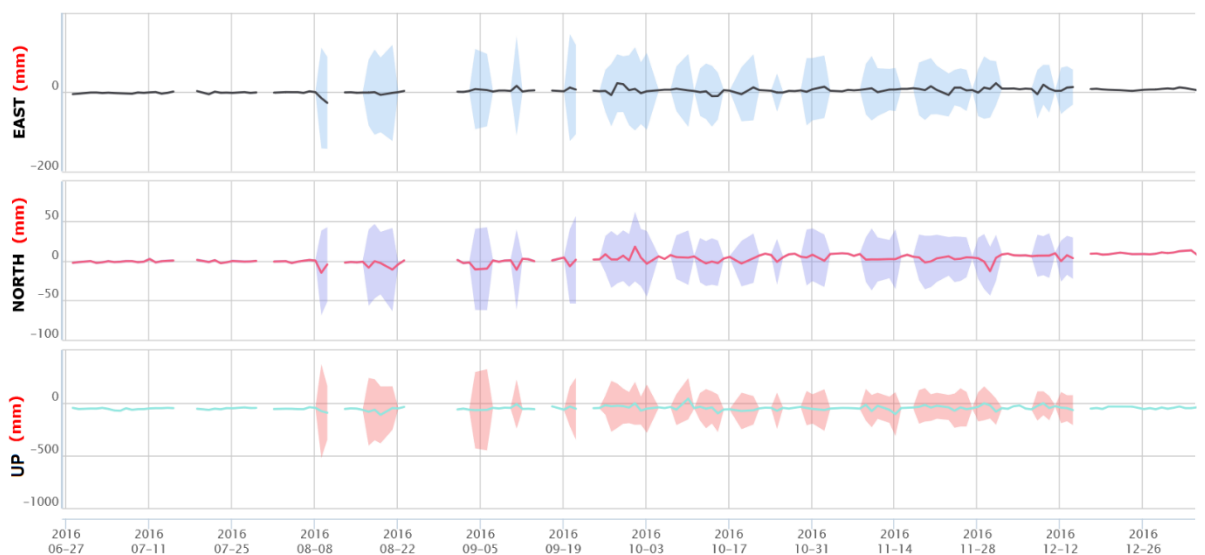


Figure 4.7. Multipath time-series of east, north and up components in 2016 belonging to MAYG station.

The east, north and up components specified in Figure 4.6 and Figure 4.7 belong to the MAYG station. GAMIT valuation was made between 26 March 2014 and 20 October 2016. Since the multipath values of these days are the highest (0.47 m – 1.13 m), the position changes were analyzed between these dates. Moreover, this station located on the African tectonic plate was chosen because of the high multipath error.

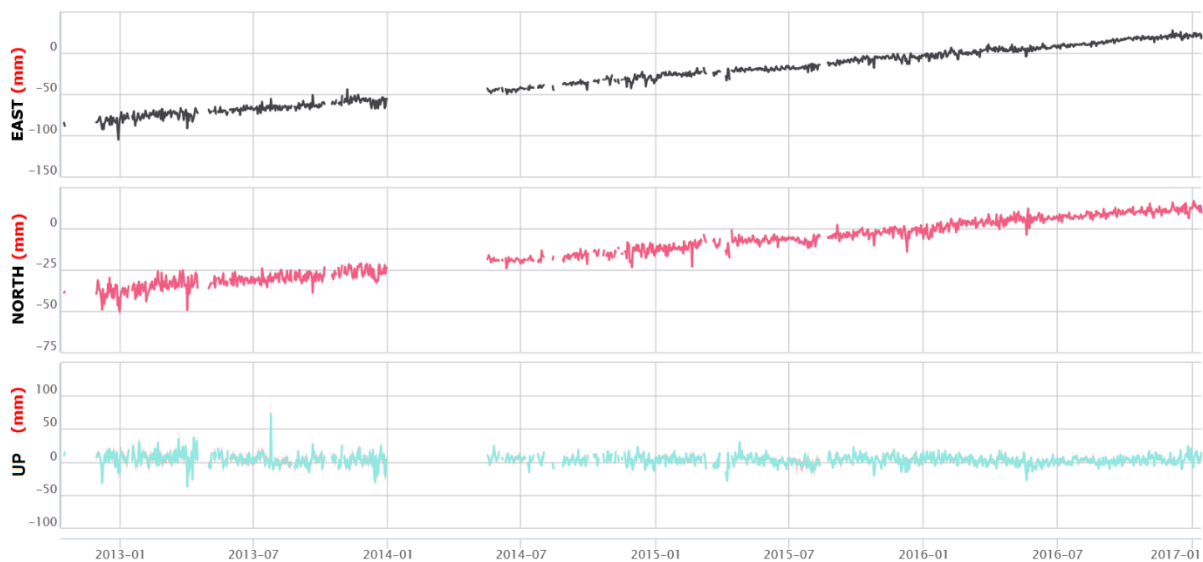


Figure 4.8. Multipath time-series of east, north and up components of SEYG station.

The east, north and up components specified in Figure 4.8 belong to the SEYG station. GAMIT evaluation was made between 27 March 2014 and 11 October 2016. Since the multipath values of these days are the highest (0.45 m – 2.22 m), the position changes were analyzed between these dates. Moreover, this station located on the African tectonic plate was chosen because of the high multipath error.

In the GAMIT evaluation, the days with the highest MP1-RMS and MP2-RMS values were chosen from the daily GPS data of the selected stations. Time-series graphs were created to investigate the effects of these RMS values on the position component. Those days which provides information about the anomalies of the selected stations in those periods were shown in Figure 4.9.

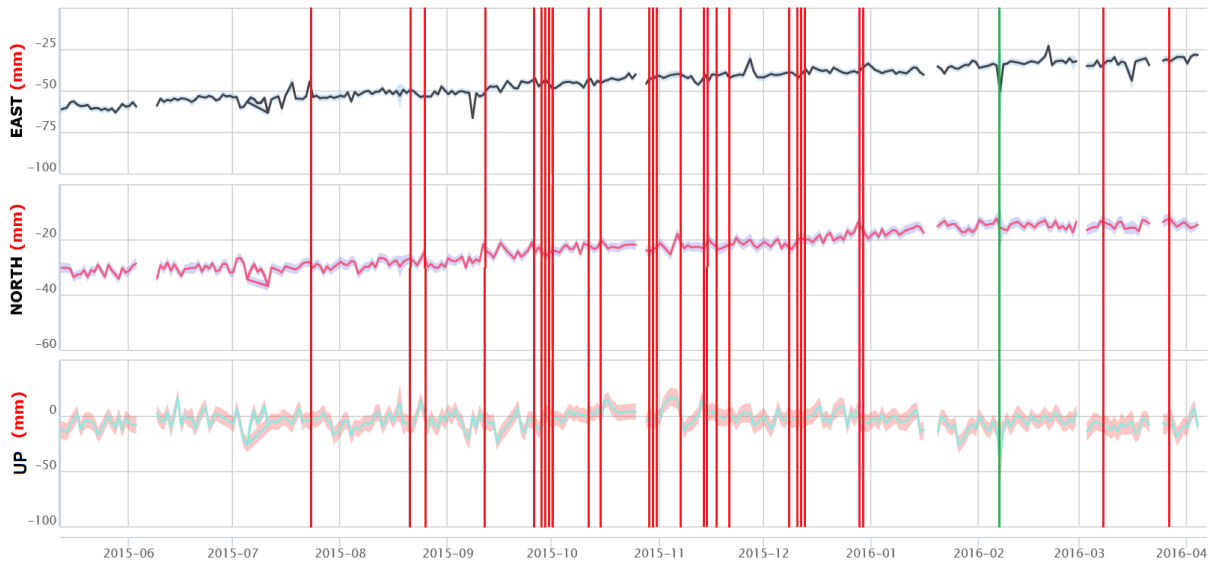


Figure 4.9. Days of the highest multipath values in the multipath time-series graph of the DJIG station.

Days that are the highest MP1-RMS and MP2-RMS values belonging to the DJIG station have been processed onto the time-series graph and these are shown in the red color as seen in Figure 4.9. It is observed that the ups and downs in all component are more severe on these days. On 29 October 2015, the elevation cut-off angle is reduced from 3° to 0° . It is seen that this change caused a disruptive effect in the last days of October 2015 on time series. In comparison to the multipath chart from the IGS website and the values calculated with TEQC software can be seen with a green line on February 4, 2016, as shown in Figure 4.10, which is badly affected by the multipath error.

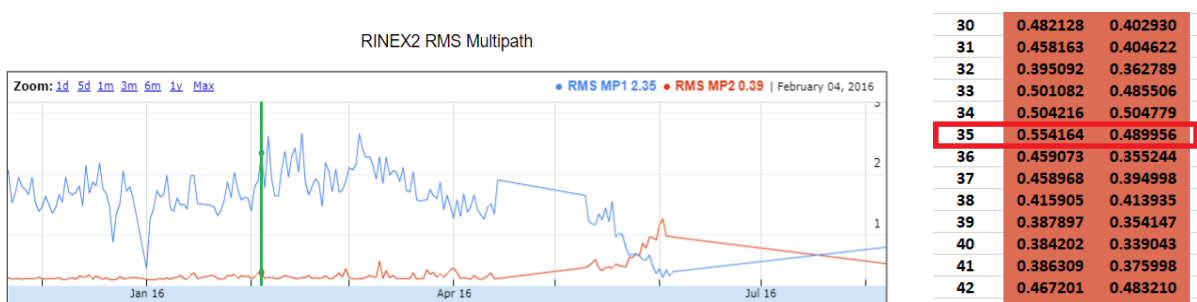


Figure 4.10. The multipath graph of DJIG station at IGS Network Site Page and high RMS value in the RMS table of the DJIG station

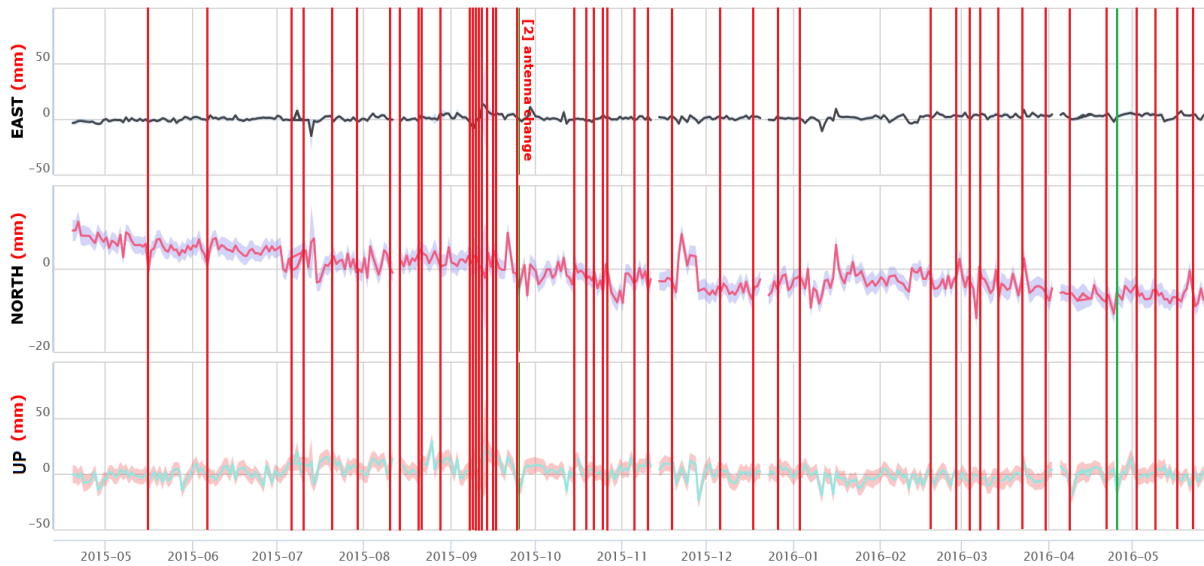


Figure 4.11. The multipath graph of DJIG station at IGS Network Site Page and high RMS value in the RMS table of the DJIG station.

Days that are the highest MP1-RMS and MP2-RMS values belonging to the DYNG station have been processed onto the time-series graph and these are shown in the red color as seen in Figure 4.11. Due to the installation of a new antenna on September 25, 2015, it caused negative effects as seen in the time-series graph. In particular, there is a noticeable difference in gray values of all components. The reason for happening the fluctuations in the last days of October 2015 is to reduce the elevation cut-off angle from 3° to 0° . As shown in Figure 4.12, due to the presence of a reflective surface around the southwest of the antenna, the quality of signals is affected poorly.



Figure 4.12. The panoramic view around the receiver of the DYNG station.

Data outages occurred on 317 and 320 days of 2015 because of the unavailability of this station. In comparison to the multipath chart from the IGS website and the values calculated with TEQC software can be seen with a green line on April 23, 2016, as shown in Figure 4.13, which is badly affected by the multipath error.

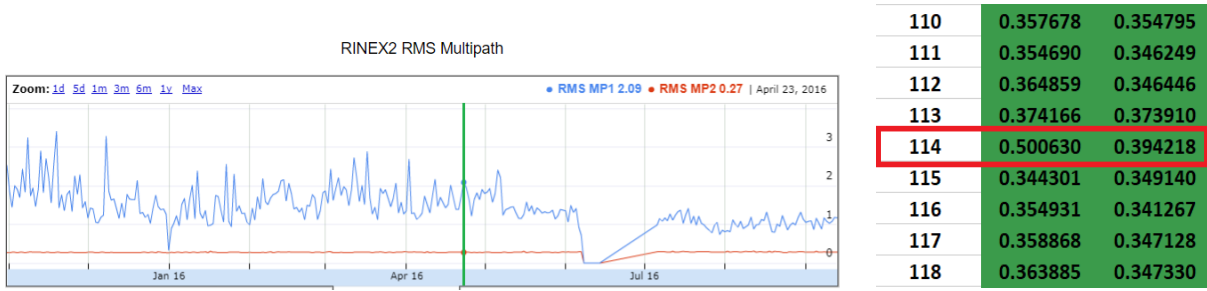


Figure 4.13. The multipath graph of DYNG station at IGS Network Site Page and high RMS value in the RMS table of the DYNG station.

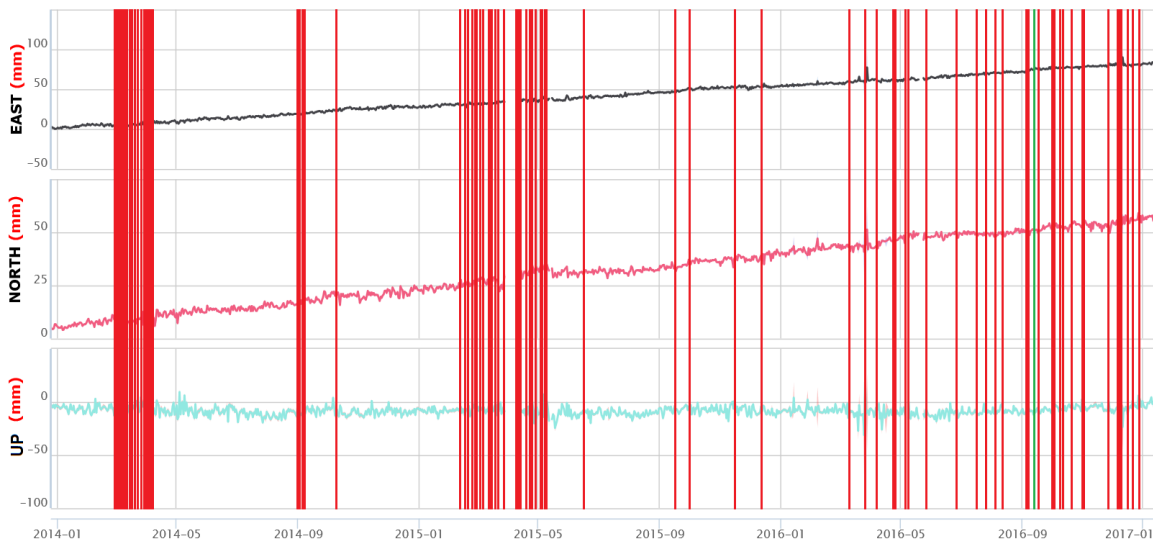


Figure 4.14. Days of the highest multipath values in the multipath time-series graph of the MAL2 station.

Days that are the highest MP1-RMS and MP2-RMS values belonging to the MAL2 station have been processed onto the time-series graph in the above and these are shown in the red color. When compared to the analysis of the other stations being processed, it is seen that the values of this station are more stable. On October 18, 2016, the firmware update of the receiver was performed. The receiver was upgraded from 2.9.0 to 2.9.5. Therefore, the fluctuations occurred that day. There are two main reasons why these days are badly affected by the multipath error. The first reason is the presence of antennas with more than one reflective surface around the antenna, as shown in Figure 4.15.



Figure 4.15. The presence of the reflective surfaces around the receiver of the MAL2 station.

The other one is that during the evaluation period (2014 January-2016 January), the performance of the station is not good as shown in Figure 4.16.

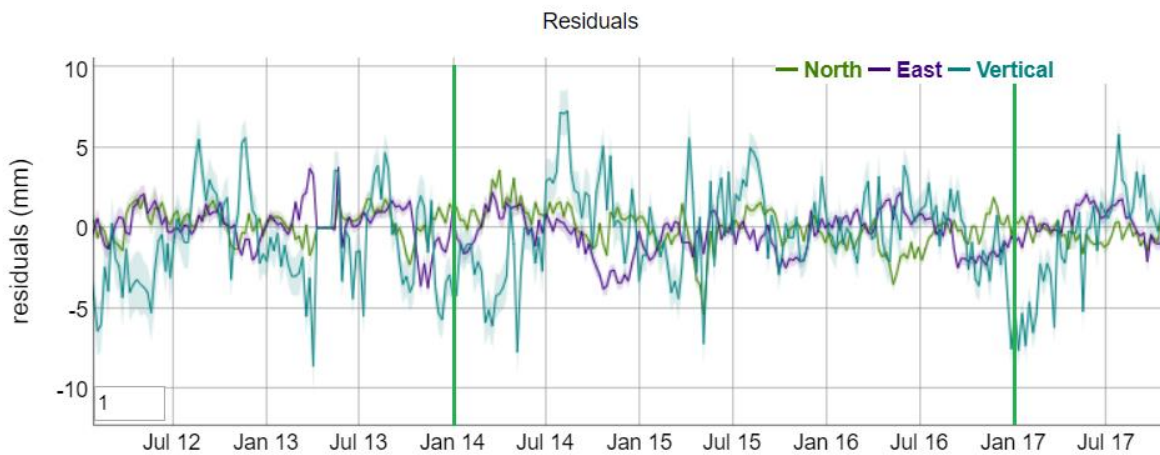


Figure 4.16. The residuals graph of MAL2 station at IGS Network Site Page

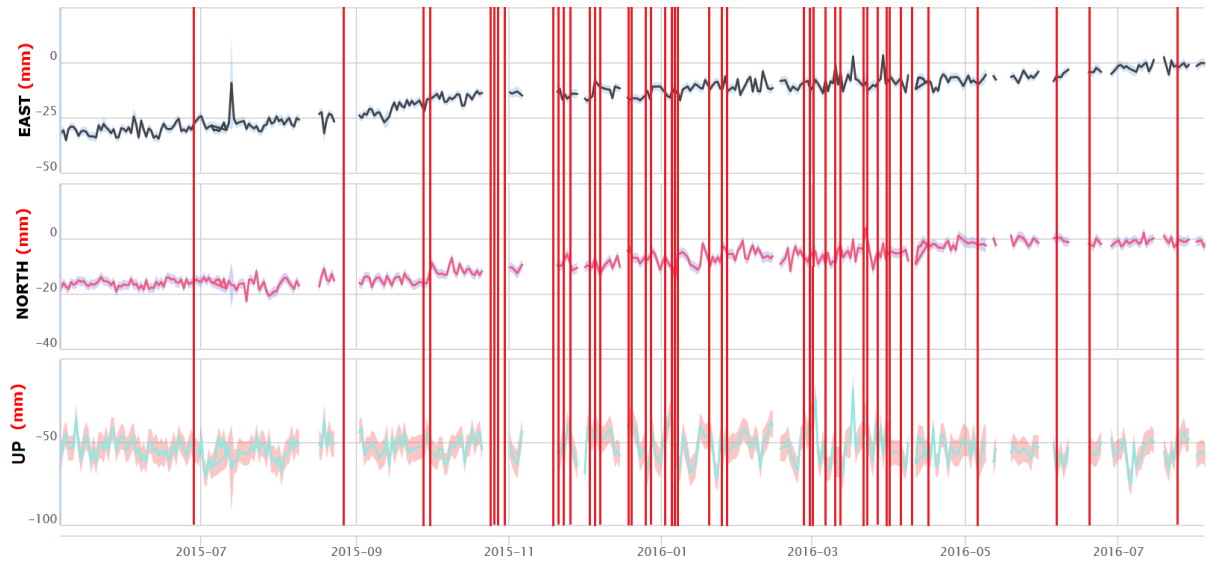


Figure 4.17. Days of the highest multipath values in the multipath time-series graph of the MAYG station in 2015 and 2016.

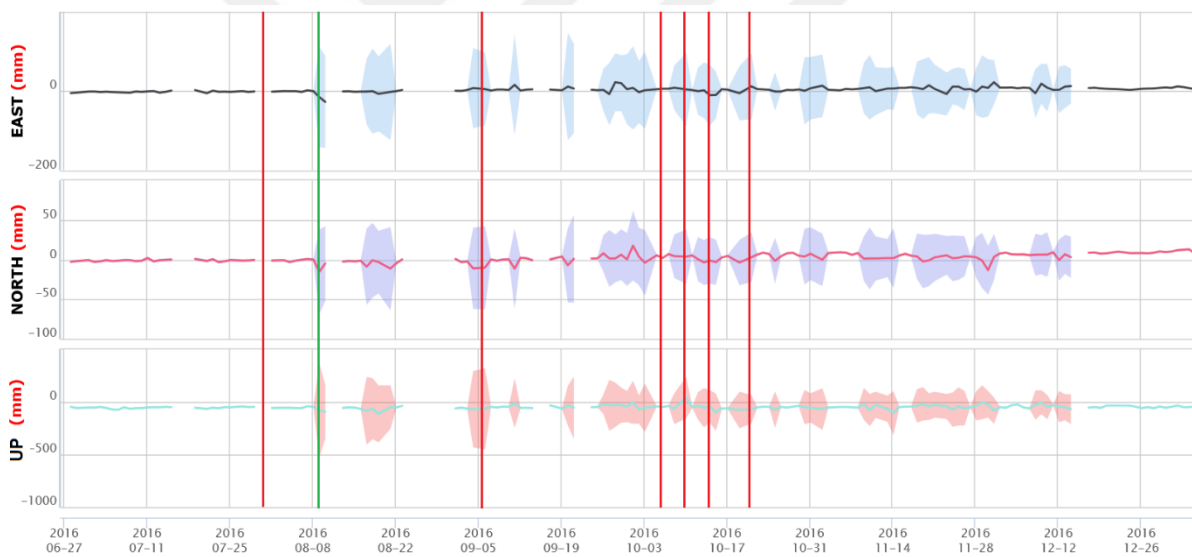


Figure 4.18. Days of the highest multipath values in the multipath time-series graph of the MAYG station in 2016.

Days that are the highest MP1-RMS and MP2-RMS values belonging to the MAYG station have been processed onto the time-series graph in Figure 4.17, Figure 4.18 and these are shown in the red color. It is seen that there are more data outages in comparison to other process stations. This is caused by the internet outage and the possible antenna issues. These days are 29 October-31 October 2015, 9 November 2015, 17 May, 8 June, 11 June, 12 June, 17 July, 14 August, 25 August 2016, 21 September-25 September 2016, 4 October 2016, 2 December-26

December 2016, 31 December 2016. On August 9, 2016, the firmware version of the receiver was upgraded from 5.01 to 5.14. This change is shown a green line in the time-series graph. Weighted root mean square values of this station is more severe in comparison with the values of the other process stations. There are two main reasons of this severest value. One of them is that the antenna was installed on the seaside as seen in Figure 4.19, Figure 4.20 and other reason is sea-level changes. (Jin et.al.2017).



Figure 4.19. East and south view around the receiver of the MAYG station.



Figure 4.20. West and north view around the receiver of the MAYG station.

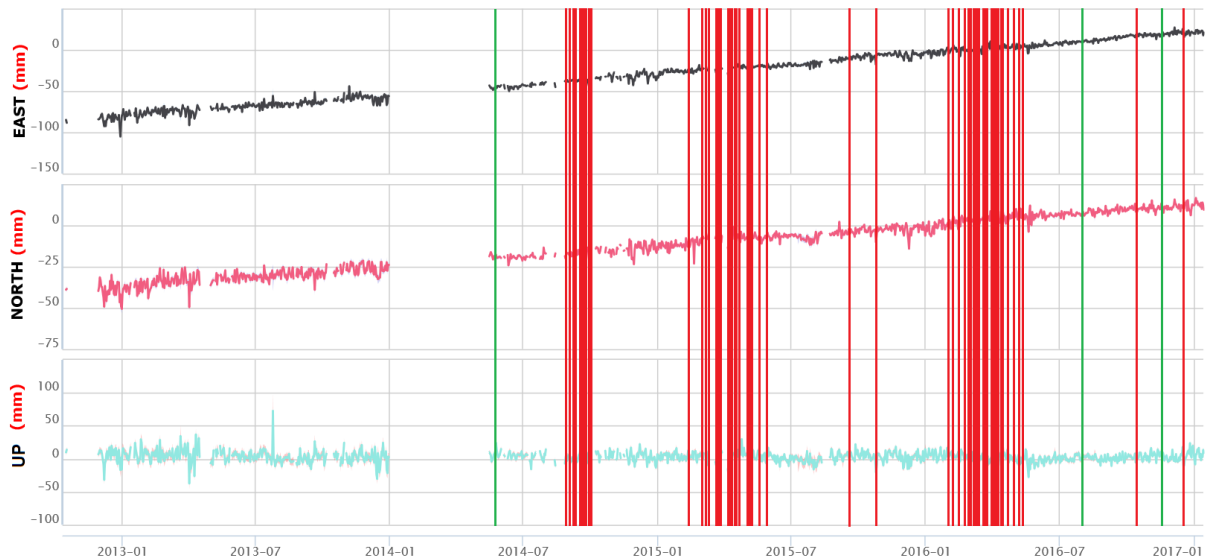


Figure 4.21. Days of the highest multipath values in the multipath time-series graph of the SEYG station.

Days that are the highest MP1-RMS and MP2-RMS values belonging to the SEYG station have been processed onto the time-series graph in Figure 4.21 and these are shown in the red color. There is no data in the vast majority of the first half of 2014 as seen in Figure 4.21. On June 16, 2014, the receiver firmware has been updated as shown with a green line in the time-series graph. In addition, the firmware version of the receiver has been updated 2 times as shown with a green line in the time-series graph. The first, on August 10, 2016, the firmware version of the receiver has been updated from 5.01 to 5.14. The second, on December 16, 2016, the firmware version of the receiver has been updated from 5.14 to 5.15. Furthermore, there is no information about the environment surrounding the antenna. Besides, during the evaluation period, the quality of the station is not good as seen in Figure 4.22.

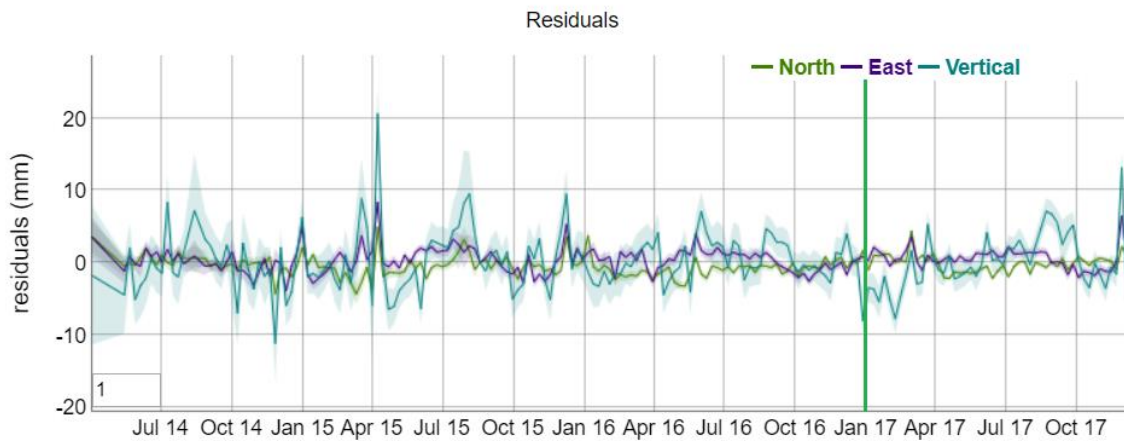


Figure 4.22. The residuals graph of SEYG station at IGS Network Site Page.



CHAPTER 5

CONCLUSIONS AND DISCUSSION

GNSS is satellite assessment system which indicates a user's location at anytime and anywhere and depends on the evaluation of code phase arrival time of at least 4 satellites. (Hofmann-Wellenhof et.al 1994) Constantly operating reference station networks of these systems are very important systems in gathering highly-accurate real-time locational information.

Although the popular one is GPS belonging to the USA, with GLONASS belonging to Russia, these two services form GNSS. (El-Rabbany 2002) The location detection systems are effectively used for many military and civil services like environment and city planning, land use, engineering and infrastructure services, multipurpose cadastral, vehicle tracking systems, search and rescue, personal mobile applications. (URL-1) Although it is widely used in many fields, the desired accuracy cannot be provided because of systematic satellite clock error, satellite orbit error, receiver clock error, ionospheric and tropospheric delays, carrier phase ambiguity (Âdâm et.al. 2002) and random errors (NCHRP 2002) which affect GNSS. Many of those errors can be removed thanks to differential techniques. However, as multipath is an unremovable error source, it is a very important error source.

Multipath (signal reflection) arises from reflections or refractions resulting from roofs, trees, metal buildings, water surfaces. (Jin et.al 2014) Reflected signals arrive later than direct signals. This relative time lag is one of the defined parameters to understand the characteristics of multipath. In this thesis, the effect of multipath error in GPS and GLONASS satellite systems is studied through analyzing time-series of chosen stations in the study zone.

Geodetic Network; it is compared to points included in IGS Network (DJIG, MAL2, MAYG, SEYG) and EUREF, which has permanent GPS station DYNG. The main reason for choosing these stations is their high probability of being affected by the multipath error. For example, DJIG station's being on a rocky region, having an object big and reflective enough a

the southeast side of the station's aerial, having more than one antenna around station's antenna, having built MAYG station very close to the sea surface and having all those stations on a tectonic plate can be shown among these reasons.

Observatory data sets, which were used in the study, were taken from CDDIS-global data bank (URL-3) and this study includes the years between 2014-2016.

TEQC software, which was supplied by UNAVCO, was used to analyze multipath errors of stations. In GNSS observatory data which is in RINEX format and has 30 seconds exemplifying ratio of 24 hours. In order to eliminate the effects of tropospheric delays and ionospheric delays of satellite receiver clock errors by using both linear combinations of the pseudo-ranges and carrier phase observations. (Estey et al. 1999, Hilla et al. 2002) Daily multipath changes (RMS-MP1 and RMS-MP2) evaluated for every one of the stations. (teqc +qc djig0010.16o).

Trimble Netr9 and Sept Polarx4 are different versions of receiver types of stations used in this study and the antennas of these stations consist of 2D or 3D choke ring antennas diminishing the multipath error. Time-series of each station between 2014-2016 were formed by using multipath error values and each was evaluated one by one. Apart from this in order to summarize multipath error value histogram graphs were drawn.

When the results of DJIG station, which is located in Djibouti and SOMALI tectonic plate, were examined. It can be seen that in 2016 RMS data of both GPS and GLONASS were high. (see Table 3.3) Especially RMS-MP1 and RMS-MP2 values of GLONASS are three times bigger than the RMS values of GPS. Besides this, in 3 years' time, DJIG station was mostly affected by the multipath error. As this station has a very rugged surrounding, it is believed to have an F-mode of multipath geometrical types.

When examined carefully it is understood that DYNG station, which is in Greece on a Eurasian tectonic plate, is less affected by multipath error when compared with the other stations. (see Table 3.3, Figure 3.1) It is believed to be a BA-mode multipath geometrical type as it is seen in Figure 5.1. It has some kinds of objects which have reflective surfaces and some kinds of buildings whose functions we don't know.



Figure 5.1. Some kind of reflective surfaces around the receiver of DYNG station.

Obvious anomalies can be seen in RMS table and time-series of MAL2 station, which is founded in Kenya and an Africa tectonic plate. (see Table 3.3, Figure 3.1) It is seen that fluctuations were more severe between 2014-2015, in 2016 this fluctuation decreased. When two systems were compared in 2014 RMS-MP2 value of GPS is three times bigger than RMS-MP2 value of GLONASS. (see Table 3.3) RMS-MP1 value of GLONASS is a bit higher than RMS-MP1 value of GPS. (see Table 3.3) RMS-MP2 value of GPS and RMS-MP2 value of GLONASS can be said as identical in 2015. (see Table 3.3) GLONASS RMS-MP1 value is a little bit bigger than GPS RMS-MP1. (see Table 3.3) GPS RMS-MP2 value is a little bit bigger than GLONASS RMS-MP2 value in 2016. GLONASS RMS-MP1 value is a little bit bigger than GPS RMS-MP1 value. MAL2 station is thought to be F-mode and BA-mode as it has more than one reflective antenna around it.

MAYG station, which is in Mayotte and an Africa tectonic plate, has higher GPS RMS-MP1 and GPS RMS-MP2 values than GLONASS RMS values. GPS values are twice as big as GLONASS values. But when looked at 2016 values, it was understood that they were alike. This shows that the RMS values of both systems were affected by multipath errors equally. In the study of Jin and others, it was stated that stations which were built near sea level have F-mode multipath geometrical type. As a result of this, it was concluded that MAYG station has also F-mode multipath geometrical type.

In SEYG station which was founded in Pointe Larue in Seychelles and an Africa tectonic plate, RMS values of both systems were affected from multipath erroring different ratios. On studying RMS values, it is understood that in 2014 GPS RMS-MP1 and GPS RMS-MP2 are six times bigger than GLONASS RMS values. During the applications when compared with other stations, the most affected year is 2014. Although in 2015 GPS RMS-MP1 and GPS RMS-MP2 values were more affected, in 2016 GLONASS RMS-MP1 and GLONASS RMS-MP2 values were more affected. As there was no information about station antenna, there was no assumption about what kind of multipath geometrical type it had.

In time-series graphs and RMS tables it can be seen that all these stations in these two systems RMS-MP1 and RMS-MP2 values show different attitudes within 3 years time. In stations with high RMS values factors like the existence of intensive signal reflection, low receiver performance, bad weather conditions, their being on tectonic plates may have negative effects. It can be seen that values belonging to stations show no normal distribution but different ones. This situation makes it difficult to explain multipath error behavior. In short, the effect of the multipath error is thought to be very complicated and it is concluded that this effect is directly related to the topography of the station antenna.

In this study in the geodetic network which was founded as follows the effect of multipath errors on position component was investigated. (see Figure 4.1) According to this, the days on which RMS values were on the highest points were determined and position components were evaluated. The evaluations were made by using GAMIT software which was developed by MIT.

In this study in order to investigate the effect of multipath errors on position component, eleven stations of IGS, which have good performance and stability, were included in the analysis. These were DGAR, ABPO, ZAMB, MBAR, ORID, GRAZ, BUCU, MIKL, ZECK, ARUC, TEHN _ all in the study area. As a result of this analysis which was made thanks to GAMIT software long period of 2014-2016 time-series were achieved in this study which includes the effects of multipath error in the north, east and up in GPS belonging to the chosen stations. When time-series belonging the stations were evaluated, it is seen that all components were affected and especially the up component was the most affected one.

When each station is evaluated in details, the repeatability values in the east component are shown in black, the repeatability values in the north component are shown in pink, and the repeatability values in the up component are shown in blue as shown in Figure 5.2. In addition to that residual values of the station are presented in grey. In time-series graph of DJIG station, it is seen that in up component multipath variations are more affected. (see Figure 5.2) In the north and up components belonging to DYNG stations in weighted root mean square values fluctuations are more, in weighted root mean square values in the east component these fluctuations are less. Existence of reflective surfaces of the station antenna in the southwest side can explain the effects of multipath in these components.

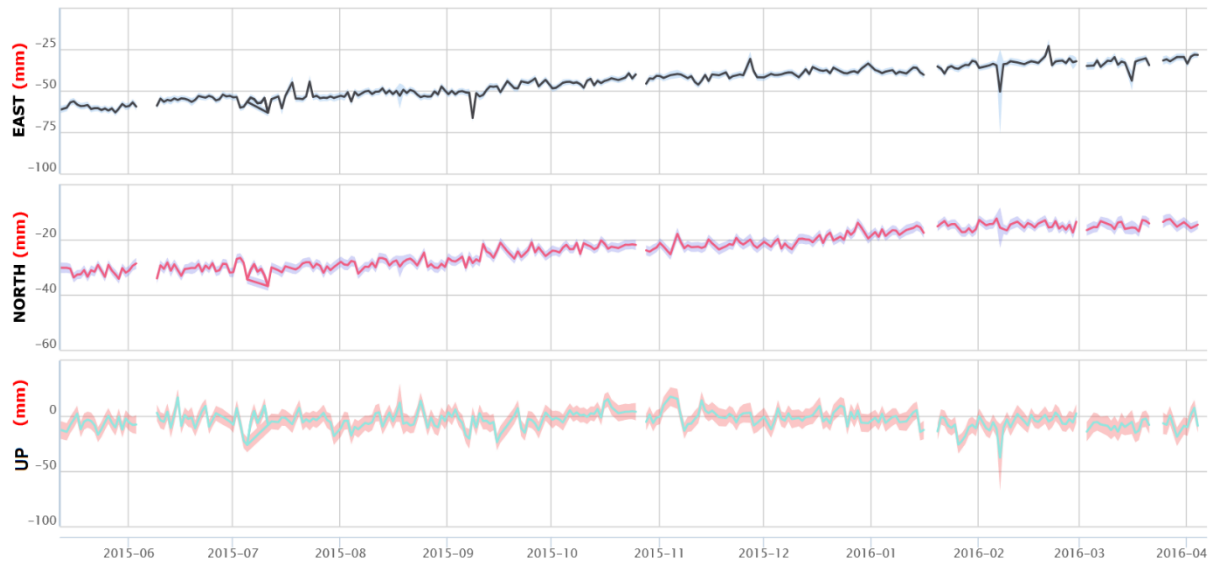


Figure 5.2. Time-series graph of DJIG station obtained by GAMIT software.

When weighted root mean square values of east, north and up components belonging to MAL2 station are compared with other stations analysis, it can be seen that it is more stable. But in some periods a serious increase was observed in all components. The reason for this is having lots of reflective objects around the station antenna, which cause multipath and this affected the quality measurements.

There happened serious fluctuations in weighted root mean square values of the east, north and up components belonging to MAYG station. It is assumed that station antenna is being built near the sea and it is getting affected by sea-level changes might have resulted in changes in the time-series graph. Moreover, it is seen that grey values are higher in all components but weighted root mean square values are more stable. It is thought that an increase happened in grey values as a result of the bad performance of the station.

The days on which the highest MP1-RMS and MP2-RMS values belonging to SEYG station are shown in the time-series graph. In the time-series graph most of the time in the first half of 2014 there was no data. On June 16, 2014 receiver firmware version was updated and it was shown as a green line in time series graph. (see Figure 4.21) Besides this receiver firmware version was updated twice more. The first one August 10, 2016 receiver firmware version was updated from 5.01 to 5.14. The second one on December 16, 2016, it was updated from 5.14 to 5.15. There is no available information about the environment surrounding the station antenna.

As seen in all stations' time-series graph, there is loss of data in some time periods. Internet cut-offs and probable antenna problems caused this. It is seen that in some certain periods diminishing the elevation cut-off from 3° to 0°, erecting a new antenna, updating or increasing receiver firmware caused a destructive effect on time-series graphs.

After examining time-series graphs belonging to the station thanks to GAMIT and TEQC software, it can be said that multipath error has a complex structure and it is mostly related to GNSS antenna surrounding. Having reflective surfaces around the antenna and their being close to each other have effects on the time-series graph of long-term multipath changes. In addition to this, it also has different effects on local meteorological effect, tectonic plate movements, seawater streams, snow effect on the radome material, local refraction effect, earthquake effect, ocean loading effect etc. (Kara 2009) The existence of such kinds of multipath errors lessens the sensitivity of positioning GPS and GLONASS systems. For this reason, it is thought that data's being formed of long-term series contributes a lot to get a better result. General judgments which are used to eliminate multipath effect are using qualified antenna like choke ring and erecting important GNSS receivers away from reflective objects. But as the cost of qualified antennas is very high, this is not always possible.

Consequently, under the light of information we gathered at the end of this study, for future similar studies on this thesis;

- Investigating the effect of multipath on a different type of facilities except for concrete pillar and metal bent bar,
- Studying the effects on elevation and azimuth angles,
- Examining different satellite systems,
- Investigating the effect of multipath on the tectonic plate movements which are on spots can be included in the study

It has been thought that more specific and comprehensive researches can be done by including the above thoughts to the studies.

REFERENCES

- Akos D M, Weiss J P, Murphy T and Pullen S** (2004) Airborne Multipath Investigation via a GPS Software Receiver, *Proceedings of the 17th International Technical Meeting of the Satellite Division of The Institute of Navigation*, 21-24 September 2004, Long Beach, CA, 1822-1831.
- Axelrad P, Gold K and Madhani P** (1999) Analysis of Orbit Errors Induced by Multipath for the ICESat Observatory, University of Colorado, Colorado Center for Astrodynamics Research, 19 March 1999, Boulder, CO.
- Beutler G** (2005) *Methods of Celestial Mechanics: Volume I: Physical, Mathematical, and Numerical Principles (Astronomy and Astrophysics Library)*, ISBN: 978-3-642-14857-6, Springer Berlin Heidelberg New York, 466
- Bétaille D, Maenpa J, Euler H J and Cross P A** (2003) New Approach to GPS Phase Multipath Mitigation, *Proceedings of the 2003 National Technical Meeting of The Institute of Navigation*, 22-24 January 2003, Anaheim, California, USA, 243-253.
- Bilich A** (2006) Improving the Precision and Accuracy of Geodetic GPS: Applications to Multipath and Seismology, *PhD Thesis*, University of Colorado, Department of Aerospace Engineering Sciences, 353.
- Bilich A and Larson K M** (2007) Mapping the GPS Multipath Environment Using the Signal-to-ratio (SNR), *Radio Sci*, 42:RS6003, Doi:10.1029/2007RS003652.
- Bishop G J, Coca D S, Kappler P H and Holland E A** (1994) Studies and Performance of a New Technique for Mitigation of Pseudorange Multipath Effects in GPS Ground Stations, *In Proceedings of the National Technical Meeting of the Institute of Navigation*, 24-26 January 1994, San Diego, CA, 231-242.
- Booth J, Murphy T, Clark B and Liu F** (2000) Validation of the Airframe Multipath Error Allocation for Local Area Differential GPS, *Proceedings of the IAIN World Congress and 56th Annual Meeting of the Institute of Navigation*, 26-28 June 2000, San Diego, CA 689-698.
- Braasch M M** (1992) On the Characterization of Multipath Errors in Satellite-Based Precision Approach and Landing Systems, *PhD Thesis*, Ohio University, The Faculty of the College of Engineering and Technology, 203.
- Brenner M, Reuter R and Schipper B** (1998) GPS Landing System Multipath Evaluation Techniques and Results, *Proceedings of the 11th International Technical Meeting of the Satellite Division of The Institute of Navigation*, 15-18 September 1998, Nashville, TN, 999-1008.

REFERENCES (continued)

- Brown A and Gerein N** (2001) Test Results from a Digital P(Y) Code Beam steering Receiver for Multipath Minimization, *Proc. ION 57th Annual Meeting*, 11-13 June 2001, Albuquerque, NM, 872-878.
- Byun S H, Hajj G A and Young L E** (2002) Assessment of GPS Signal Multipath Interference, *Proceedings of the 2002 National Technical Meeting of the Institute of Navigation*, 28-30 January 2002, San Diego, CA, 694-705.
- Chang L C and Juang J C** (2008) An Adaptive Multipath Mitigation Filter For GNSS Applications, *EURASIP Journal on Advances in Signal Processing*, Volume 2008:10, Doi: 10.1155/2008/214815.
- Comp C J and Axelrad P** (1998) Adaptive SNR-based Carrier Phase Multipath Mitigation Technique, *IEEE Trans Aerospace Electron System* 34(1):264-276, Doi:10.1109/7.640284,
- Counselman C and Gourevitch S** (1981) Miniature Interferometer Terminals for Earth Surveying: Ambiguity and Multipath with Global Positioning System, *IEEE Transactions on Geoscience and Remote Sensing*, GE-19(4):244-252, Doi: 10.1109/TGRS.1981.350379.
- Elosegui P, Davis J L, Jaldehag R T K, Johansson J M, Niell A E and Shapiro I I** (1995) Geodesy Using the Global Positioning System: The Effects of Signal Scattering on Estimates of Site Position, *Journal of Geophysical Research: Solid Earth*, 100(B6), 9921-9934, Doi: 10.1029/95jb00868.
- El Rabbany A** (2002) *Introduction to GPS: The Global Positioning System*”, Artech House, ISBN: 1-58053-183-0, Boston, London.
- Estey L H and Meertens C M** (1999) TEQC: The Multi-Purpose Toolkit for GPS/GLONASS Data, *GPS Solution* 3(1):42-49, Doi:10.1007/PL00012778.
- Georgiadou Y and Kleusberg A** (1988) On Carrier Signal Multipath Effects in Relative GPS Positioning, *Manuscripta Goedaetica*, 13(3):172-179.
- Ge L L, Han S W and Rizos C** (2000a) Multipath Mitigation of Continuous GPS Measurements Using an Adaptive Filter, *GPS Solution* 4(2):19-30, Doi:10.1007/PL00012838.
- Ge L L, Han S W and Rizos C** (2002) GPS Multipath Change Detection in Permanent GPS Stations, *Survey Review* 36(283):306-322, Doi: 10.1179/003962602791483271.
- Hannah B M** (2001) *Modelling and Simulation of GPS Multipath Propagation*, *PhD Thesis*, Queensland University of Technology, Australia, 284.
- Hagerman L** (1973) Effects on Multipath of Coherent and Non-coherent PRN Ranging Receiver, *Aerospace Report No: TOR-0073(3020-03)-3*, Development Planning Division, The Aerospace Corporation, 39.

REFERENCES (continued)

- Herring T A, King R W, Floyd M A and McClusky S C** (2015) Introduction to GAMIT/GLOBK, Massachusetts Institute of Technology, Department of Earth, Atmospheric, and Planetary Sciences, 50.
- Hilla S and Cline M** (2002) Evaluating Pseudo-range Multipath Effects at Stations in The National CORS Network, The Ohio State University, Weikko A., Heiskanen Symposium in Geodesy, 1-4 Oct 2002, Columbus, OH.
- Hilla S and Cline M** (2004) Evaluating Pseudo-range Multipath Effects at Stations in The National CORS Network, *GPS Solutions*, 7(4):253-267, Doi: 10.1007/s10291-003-0073-3.
- Hofmann-Wellenhof B, Lichtenegger H and Collins J** (1994) Global Positioning Systems: Theory and Practice, 5th edition, ISBN: 3211835342, Springer-Verlag Wien, Doi: 10.1007/978-3-7091-3311-8.
- Jin S G, Feng G P and Gleason S** (2011) Remote Sensing Using GNSS Signals: Current Status and Future Directions, *Advances in Space Research*, 47(10):1645-1653, Doi: 10.1016/j.asr.2011.01.036.
- Jin S G, Van Dam T and Wdowinski S** (2013) Observation and Understanding the Earth System Variations from Space Geodesy, *Journal of Geodynamics*, 72:1-10, Doi: 10.1016/j.jog.2013.08.001.
- Jin S G, Cardellach E and Xie F** (2014) GNSS Remote Sensing Theory, Methods and Applications, 1st edition, 19, ISBN: 978-94-007-7482-7, Springer Dordrecht Heidelberg, New York, London, 276, Doi: 10.1007/978-94-007-7482-7.
- Jin, S G, Qian X and Wu X** (2017) Sea Level Change from BeiDou Navigation Satellite System-Reflectometry (BDS-R): First Results and Evaluation, *Global and Planetary Change*, Doi: 10.1016/j.gloplacha.2016.12.010.
- Kahveci M and Yıldız F** (2012) GPS/GNSS Satellite Positioning Systems Theory and Practice (in Turkish), ISBN 978-605-133-265-9, Nobel Akademik Yayıncılık Eğitim Danışmanlık Tic. Ltd. Şti., Ankara, 280.
- Lachapelle G, Julien O, MacGougan G, Cannon M E and Ryan S** (2003) Ship GPS Multipath Detection Experiments, *Proceedings of the 59th Annual Meeting of The Institute of Navigation and CIGTF 22nd Guidance Test Symposium*, 23-25 June 2003, Albuquerque, NM, 217-229.
- Leick A** (2004) GPS Satellite Surveying, 3rd edition, ISBN 0-471-05930-7, John Wiley Sons, Inc., New Jersey, 464.
- Lippincott W L, Milligan T and Igli D** (1996) Method for Calculating Multipath Environmental and Impact on GPS Receiver Solution Accuracy, *Proceedings of the 1996 National Technical Meeting of The Institute of Navigation*, 22-24 January 1996, Santa Monica, CA, 707-722.

REFERENCES (continued)

- Mekik C and Can O** (2010) Multipath Effects in RTK GPS and A Case Study, *Journal of Aeronautics, Astronautics and Aviation, Series A*, 42(4):231-240.
- Montenbruck O, Helleputte T, Kroes R and Gill E** (2005) Reduced Dynamic Orbit Determination Using GPS Code and Carrier Measurements, *Aerospace Science and Technology*, 9:261-271.
- Murphy T, Snow R and Braasch M** (1996) GPS Multipath on Large Commercial Air Transport Airframes, *Navigation Journal of the Institute of Navigation*, 43(4):397-406, Doi: 10.1002/j.2161-4296.1996.tb01928.x.
- Murphy T, Friedman R, Booth J, Geren P, Molloy N, Clark B and Burns J** (2004) Program for the Investigation of Airborne Multipath Errors, *Proceedings of the 2004 National Technical Meeting of The Institute of Navigation*, 26-28 January 2004, San Diego, CA, 781-792.
- Murphy T, Harris M, Geren P, Pankaskie T, Clark B and Burns J** (2005) More Results from the Investigation of Airborne Multipath Errors, *Proceedings of the 18th International Technical Meeting of the Satellite Division of The Institute of Navigation*, 13-16 September 2005, Long Beach, CA, 2670-2687.
- Park K D, Nerem R S, Schenewerk M S and Davis J L** (2004) Site-Specific Multipath Characteristics of Global IGS and CORS GPS Sites, *Journal of Geodesy*, 77(12):799-803.
- Tiryakioğlu I, Güllü M, Baybura T and Erdoğan S** (2005) GPS Points to Signal Reflection Effective Investigation, 2 Engineering Measurements Symposium, 23-25 November 2005, İstanbul, Türkiye, 10.
- Tiryakioğlu I, Taktak F and Çetintaş F** (2006) GPS Signal Multipath Error and Elimination Methods (in Turkish), ISSN: 1305-631X, Yapı ve Teknolojileri Elektronik Dergisi, 2:35-41.
- Thornberg D B, Thornberg D D, DiBenedetto M F, Braasch M S, Graas F V and Bartone C** (2003) The LAAS Integrated Multipath Limiting Antenna (IMLA), *Proceedings of the 15th International Technical Meeting of the Satellite Division of The Institute of Navigation*, 24-27 September, Portland, OR, 2082-2092.
- Transportation Research Board Executive Committee** (2002) NCHRP (National Cooperative Highway Research Program) Synthesis 301: Collecting, Processing and Integrating GPS Data into GIS, ISBN: 0-309-06916-5, National Academy Press, 65, Doi: 10.17226/25519.
- Van Nee D J R, Misser S H and Prasad R** (1992) Direct Sequence Spread Spectrum in a Shadowed Rician Fading Land-Mobile Satellite Channel, *IEEE Journal on Selected Areas in Communications*, 10(2):350-357.

REFERENCES (continued)

Van Nee D J R (1995) Multipath and Multi-Transmitter Interference in Spread-Spectrum Communication and Navigation Systems, *PhD Thesis*, ISBN: 90-407-1120-8, Delft University of Technology, The Netherlands, 208.

Yıldız S S, Yağcı A, Özkan A, Yavaşoğlu H, Altın M U and Tarı E (2009) GPS Gözlem Süresinin Yüksek Doğruluklu Çalışmalarda Zaman Serileri ve Hız Vektörleri Üzerine Etkisi, TMMOB Harita ve Kadastro Mühendisleri Odası, 12. Türkiye Harita Bilimsel ve Teknik Kurultayı, 11-15 Mayıs, Ankara, Türkiye, 5.

URL-1 <<https://www.novatel.com/an-introduction-to-gnss/chapter-8-gnss-applications-and-equipment/applications/>>, Last Visit: 29.07.2019.

URL-2 <<http://gpsworld.com/gnss-systemalgorithms-methodsinnovation-multipath-minimization-method-11849/>>, Last Visit: 29.07.2019

URL-3 <<ftp://cddis.gsfc.nasa.gov/gnss/data/daily>>, Last Visit: 29.07.2016



APPENDICES

Appendix A: RMS Data of GPS in 2014

	DJIG		DYNG		MAL2		MAYG		SEYG	
	MP1	MP2	MP1	MP2	MP1	MP2	MP1	MP2	MP1	MP2
1					0.536914	0.3188				
2										
3					0.530468	0.330566				
4					0.544917	0.372115				
5					0.554701	0.329745				
6					0.548944	0.333516				
7					0.587659	0.337899				
8					0.563563	0.331089				
9					0.524039	0.312301				
10					0.522826	0.328766				
11					0.54169	0.379993				
12					0.510397	0.316599				
13					0.531842	0.334776				
14					0.544228	0.35375				
15					0.538751	0.31581				
16					0.526927	0.318008				
17					0.512718	0.320516				
18					0.515487	0.3497				
19					0.527083	0.343508				
20					0.519288	0.330952				
21					0.552118	0.357001				
22					0.530418	0.369445				
23					0.596697	0.367311				
24					0.53629	0.304751				
25					0.564229	0.340494				
26					0.538496	0.335642				
27					0.536304	0.337738				
28					0.512286	0.318251				
29					0.542724	0.333893				
30					0.585996	0.364916				
31					0.567614	0.353679				
32					0.540574	0.340955				
33					0.542122	0.342223				
34					0.519559	0.336587				
35					0.537783	0.326486				
36					0.520542	0.318869				
37					0.50977	0.339631				
38					0.517604	0.338062				
39					0.518777	0.345824				
40					0.539222	0.318767				
41					0.540973	0.339662				
42					0.557177	0.424575				
43					0.538252	0.33148				
44					0.550558	0.348146				
45					0.55758	0.379459				
46					0.552032	0.326265				
47					0.560652	0.34219				
48					0.555383	0.354092				

49			0.525669	0.350645		
50			0.558664	0.326603		
51			0.530958	0.346032		
52			0.539491	0.325689		
53			0.537623	0.343783		
54			0.54986	0.383141		
55			0.552969	0.383445		
56			0.552203	0.389005		
57			0.561879	0.390981		
58			0.648135	0.52091		
59			0.843107	0.591435		
60			0.62072	0.485666		
61			0.592896	0.423063		
62			0.658601	0.453277		
63			0.599253	0.440523		
64			0.700753	0.50459		
65			0.588242	0.367189		
66			0.620588	0.471338		
67			0.636783	0.343885		
68			0.744982	0.582411		
69			0.629271	0.461559		
70			0.703486	0.596868		
71			0.668636	0.491866		
72			0.881321	0.63071		
73			0.822342	0.618589		
74			0.711424	0.525346		
75			0.648441	0.504887		
76			0.813551	0.676088		
77			0.842723	0.74567		
78			0.622321	0.523395		
79			0.865999	0.670995		
80			0.864725	0.749537		
81			0.803955	0.539966		
82			0.605667	0.464245		
83			0.619251	0.43702		
84			0.800962	0.568353		
85			0.718246	0.542166		
86			0.694363	0.487612		0.783468 0.604588
87			0.664874	0.522882	0.451585 0.439868	0.719537 0.637932
88			0.915235	0.577309	0.536253 0.460234	0.862648 0.750441
89			0.980237	0.878695	0.77333 0.7855	1.112519 1.144001
90			0.8093	0.610302	0.502546 0.462375	0.900649 0.893796
91			0.782336	0.573533	0.627289 0.5757	1.197265 1.168229
92			0.81913	0.742515	0.550838 0.544184	0.986153 0.988872
93			0.701307	0.533117	0.496993 0.490102	0.939531 0.918247
94			0.648904	0.489361	0.61288 0.501517	0.662687 0.623911
95			0.613604	0.47519	0.461451 0.454869	0.513684 0.449968
96			0.709117	0.510535	0.570979 0.54351	0.774865 0.752752
97			0.600241	0.41994	0.449362 0.457937	0.470843 0.431756
98			0.672135	0.470666	0.537082 0.495473	0.530928 0.539923

99			0.569924	0.485383	0.456871	0.461693	0.518244	0.441332
100			0.618708	0.381828	0.468074	0.477998	0.630049	0.498985
101			0.574845	0.413108	0.511748	0.495508	2.217913	2.19045
102			0.55467	0.332371	0.46239	0.456776	0.372896	0.356607
103			0.546832	0.342246	0.451588	0.447761	0.389997	0.357826
104			0.613491	0.467628	0.541799	0.512786	0.402413	0.364337
105			0.647822	0.484032	0.466958	0.466166	0.485795	0.485647
106			0.592814	0.433592	0.591132	0.488393	0.512717	0.516079
107			0.532454	0.358453	0.470568	0.460656	0.589495	0.46032
108			0.593763	0.429976	0.474909	0.460124	0.576327	0.497155
109			0.462259	0.466015	0.462259	0.466015	0.393654	0.372899
110			0.555788	0.3558	0.44777	0.454166	0.390326	0.361581
111			0.553466	0.382576	0.544022	0.522626	0.477032	0.433469
112			0.705337	0.478495	0.71706	0.687479	0.745874	0.542467
113			0.594372	0.373954	0.4838	0.478356	0.518522	0.490307
114			0.538339	0.37722	0.476056	0.462139	0.474128	0.413558
115			0.61913	0.459752	0.49595	0.488121	0.570597	0.405665
116			0.583297	0.423004	0.526135	0.518011	0.426733	0.366012
117			0.67043	0.366422	0.500622	0.47386	0.385672	0.367986
118			0.556767	0.372774	0.483607	0.473027	0.379814	0.361581
119			0.56199	0.400227	0.559806	0.493989	0.422591	0.40247
120			0.616914	0.44467	0.485114	0.481406	0.513417	0.376128
121			0.682171	0.387504	0.486622	0.48419	0.383389	0.362746
122			0.658857	0.443377	0.510388	0.69998	0.483708	0.446132
123			0.587884	0.419005	0.514199	0.635043	0.419788	0.42043
124			0.583939	0.386358	0.476586	0.474036	0.372519	0.358242
125			0.584213	0.386498	0.452641	0.446554	0.411695	0.358216
126			0.577821	0.411936	0.482199	0.469669	0.452505	0.415626
127			0.571305	0.434975	0.456559	0.460215	0.391293	0.363275
128			0.585342	0.38515	0.466707	0.457094	0.393185	0.359888
129			0.61099	0.360728	0.467228	0.45213	0.386141	0.375555
130			0.545054	0.342805	0.478568	0.490643	0.368941	0.356645
131			0.561622	0.365731	0.487615	0.465552	0.38182	0.348775
132			0.58049	0.387776	0.462063	0.457352	0.376964	0.357107
133			0.53735	0.359879	0.472688	0.536775	0.405929	0.367336
134			0.576129	0.339008	0.486827	0.474607	0.394007	0.385811
135			0.589613	0.463421	0.464248	0.466583	0.358532	0.351529
136			0.549068	0.340581	0.525299	0.484965	0.385996	0.352
137			0.539814	0.38402	0.477686	0.480523	0.399353	0.384271
138			0.518501	0.327323	0.452395	0.458521	0.378905	0.348172
139			0.582874	0.423635	0.486105	0.488502	0.375717	0.349874
140			0.580764	0.369022	0.46759	0.479017	0.369884	0.352777
141			0.62093	0.446793	0.471381	0.467088	0.411576	0.406861
142			0.581486	0.371956	0.453415	0.454006	0.377385	0.348745
143			0.62654	0.439169	0.489154	0.487124	0.403161	0.391938
144			0.562733	0.397687	0.475824	0.449981	0.37126	0.361032
145			0.560275	0.435027	0.443394	0.48226	0.360451	0.335708
146			0.549931	0.350284	0.449577	0.443659	0.3699	0.350083
147			0.504156	0.327375	0.529519	0.522773	0.377097	0.349215
148			0.521715	0.347804	0.479106	0.466637	0.372223	0.331806

149			0.577615	0.388542	0.46613	0.455726	0.366369	0.341704	
150			0.545082	0.348529	0.452938	0.450096	0.36249	0.338344	
151			0.521766	0.351691	0.47018	0.451309	0.367461	0.356145	
152			0.522992	0.361793	0.469325	0.450317	0.374681	0.366719	
153			0.529759	0.340173	0.480815	0.481919	0.377759	0.356732	
154			0.538748	0.37591	0.502295	0.440382	0.369761	0.352657	
155			0.568861	0.341182	0.457028	0.455753	0.383296	0.356706	
156			0.613731	0.379316	0.483196	0.459436	0.374821	0.342691	
157			0.611291	0.453042	0.544696	0.495973	0.501567	0.501635	
158			0.512106	0.346938	0.468776	0.461757	0.360507	0.342861	
159		0.333175	0.328572	0.624548	0.329544	0.476685	0.461372	0.372748	0.348018
160			0.595016	0.396461	0.554887	0.473491	0.424374	0.369937	
161			0.565282	0.331681	0.526998	0.507161	0.405812	0.372412	
162			0.522695	0.351435	0.47671	0.456654	0.365965	0.341365	
163			0.573408	0.332608	0.478409	0.466007	0.371596	0.362499	
164			0.528274	0.35417	0.481187	0.465735	0.358912	0.335052	
165			0.517326	0.324502	0.475343	0.444609	0.376425	0.34428	
166			0.549203	0.366111	0.463453	0.437738	0.364138	0.344547	
167			0.566072	0.352735	0.442767	0.440967	0.373997	0.345709	
168			0.53375	0.35733	0.448693	0.446247	0.371371	0.349627	
169			0.53317	0.326972	0.439022	0.435676	0.363567	0.341163	
170			0.539199	0.349713	0.460737	0.437902	0.356876	0.337399	
171			0.540061	0.336719	0.449373	0.45933	0.368052	0.363411	
172			0.48487	0.312923	0.491844	0.485848	0.396999	0.349884	
173			0.547248	0.338111	0.455218	0.440862	0.373461	0.341985	
174			0.531763	0.364637	0.483144	0.443864	0.375838	0.351391	
175			0.547212	0.359566	0.460267	0.458155	0.368988	0.354943	
176			0.533435	0.354082	0.469126	0.45059	0.365495	0.345018	
177			0.572352	0.378932	0.456707	0.452673	0.358143	0.34468	
178			0.562251	0.342256	0.476722	0.48866	0.370062	0.344567	
179			0.56798	0.368908	0.453929	0.442927	0.37145	0.353588	
180			0.547659	0.389365	0.445818	0.438604	0.380719	0.368013	
181			0.557702	0.355077	0.486763	0.493473	0.414438	0.39214	
182			0.524735	0.340402	0.487999	0.463928	0.449342	0.458436	
183			0.547655	0.358407	0.459237	0.442719	0.359591	0.33276	
184			0.616416	0.410408	0.607007	0.62433	0.375578	0.373601	
185			0.590205	0.400359	0.54256	0.552675	0.371431	0.35946	
186			0.518836	0.354506	0.499828	0.529542	0.372017	0.398942	
187			0.525413	0.358042	0.485153	0.472532	0.38339	0.392299	
188			0.516857	0.329417	0.460182	0.451749	0.367916	0.348422	
189			0.53591	0.348413	0.520912	0.483047	0.487441	0.440365	
190			0.491299	0.332022	0.463868	0.470011	0.366227	0.354825	
191			0.503723	0.339636	0.461376	0.462133	0.383294	0.389258	
192			0.491256	0.341856	0.448767	0.440903	0.381362	0.36064	
193			0.486738	0.305042	0.487288	0.498748	0.372957	0.347388	
194			0.532767	0.33561	0.439328	0.429652	0.383169	0.368466	
195			0.512407	0.338198	0.455937	0.441594	0.360724	0.340848	
196			0.516498	0.340687	0.443127	0.445442	0.373832	0.341405	
197			0.577057	0.353321	0.467488	0.438276	0.393129	0.357602	
198			0.541591	0.387344	0.484139	0.457538	0.371899	0.348378	

199			0.569617	0.357549	0.559811	0.550427	0.372933	0.353423
200			0.52463	0.354212	0.469659	0.465694	0.369075	0.343004
201			0.560422	0.39173	0.453035	0.481093	0.367316	0.342722
202			0.541479	0.353424	0.497151	0.461887	0.378737	0.360255
203			0.522979	0.33963	0.457941	0.446388	0.377301	0.346
204			0.547553	0.32537	0.507319	0.459182	0.365568	0.363434
205			0.541472	0.339839	0.470957	0.445518	0.378261	0.358147
206			0.548696	0.334308	0.444727	0.430842	0.380853	0.353502
207			0.54092	0.351237	0.438365	0.43728	0.359121	0.34864
208			0.534359	0.343474	0.472206	0.473786	0.397045	0.370215
209			0.565176	0.389907	0.440618	0.437433	0.377141	0.357834
210			0.583022	0.334303	0.444328	0.457927	0.367241	0.344735
211			0.525005	0.363388	0.465535	0.445411	0.370891	0.339367
212			0.549471	0.395078	0.489298	0.492751	0.4026	0.367596
213			0.530169	0.36499	0.455829	0.441266	0.416976	0.419704
214			0.548694	0.402143	0.47866	0.497549	0.537614	0.510646
215			0.570199	0.409263	0.48794	0.496927	0.538267	0.499113
216			0.567735	0.341449	0.463023	0.470671	0.538267	0.499113
217			0.512847	0.342689	0.444797	0.44683	0.422905	0.40899
218			0.529276	0.353985	0.487875	0.506232	0.380683	0.350256
219			0.539127	0.366241	0.480224	0.466689	0.569899	0.438264
220			0.556148	0.405741	0.52517	0.531731	0.499599	0.503503
221			0.568015	0.41846	0.52517	0.531731	0.430097	0.373715
222			0.533712	0.351619	0.474951	0.449578	0.493583	0.397084
223			0.561113	0.335956	0.459903	0.448216	0.364421	0.347836
224			0.556132	0.358634	0.477179	0.44724	0.368411	0.354231
225			0.544305	0.351038	0.476788	0.480657	0.366984	0.356005
226			0.574196	0.388633	0.454904	0.452697	0.392509	0.369506
227			0.52161	0.357109	0.448277	0.438524	0.372202	0.352456
228			0.520779	0.341491	0.447294	0.441172	0.398474	0.344677
229			0.641424	0.387293	0.485241	0.48711	0.421339	0.400642
230			0.553452	0.378711	0.504866	0.474948	0.376453	0.366526
231			0.532437	0.358778	0.447913	0.444617	0.398534	0.408598
232			0.563274	0.355199	0.48983	0.477757	0.393502	0.349924
233			0.544878	0.351277	0.492426	0.455389	0.37788	0.357031
234			0.571389	0.378953	0.492426	0.455389	0.38948	0.397861
235	0.360869	0.333834	0.549166	0.351512	0.491768	0.472142	0.418105	0.424661
236	0.346513	0.346672	0.515996	0.38434	0.491391	0.474538	0.388201	0.378955
237	0.341339	0.334746	0.551716	0.36013	0.46296	0.470646	0.455733	0.369079
238	0.350086	0.34609	0.567583	0.334156	0.480886	0.449901	0.391031	0.37536
239	0.352632	0.365657	0.514076	0.325674	0.452454	0.448384	0.365849	0.349255
240	0.351267	0.323036	0.556562	0.359709	0.462681	0.461211	0.386495	0.364642
241	0.344182	0.333828	0.528537	0.349942	0.46534	0.485485	0.366328	0.352314
242			0.590153	0.498728	0.611987	0.6528	0.417124	0.385696
243			0.562524	0.354471	0.501331	0.471306	0.423166	0.400105
244	0.350889	0.330999	0.52804	0.331354	0.463034	0.444167	0.359805	0.349625
245	0.354163	0.342673	0.536997	0.348023	0.450199	0.457335	0.38744	0.361064
246	0.346368	0.328401	0.544434	0.360274	0.453522	0.453966	0.38523	0.37083
247	0.351834	0.337759	0.545761	0.374215	0.449164	0.45251	0.467993	0.458132
248	0.35851	0.338096	0.599469	0.348182	0.445018	0.442732	0.503736	0.474068

249	0.331906	0.327545	0.577276	0.352683	0.462328	0.444386	0.374525	0.354372
250	0.330347	0.339104	0.69486	0.494772	0.551595	0.495163	0.50971	0.545303
251	0.347543	0.347808	0.548446	0.351293	0.445024	0.456007	0.375774	0.366459
252	0.343703	0.337427	0.689757	0.517911	0.619264	0.543936	0.715331	0.718222
253	0.337161	0.339868	0.634126	0.428245	0.722614	0.555784	0.544684	0.53747
254	0.341996	0.340427	0.624334	0.399007	0.484904	0.481627	0.476535	0.428831
255	0.332582	0.349109	0.713474	0.469619	0.425081	0.787454	0.617554	0.641126
256	0.336224	0.338346	0.588405	0.419745	0.489843	0.452557	0.417256	0.373539
257	0.337672	0.340521	0.571532	0.414717	0.529514	0.497759	0.61478	0.500087
258	0.349021	0.325964	0.681953	0.506166	0.54173	0.528294	0.67137	0.508491
259	0.339884	0.324607	0.720343	0.39727	0.527646	0.487693	0.593762	0.580983
260	0.336398	0.33414	0.59524	0.446075	0.492952	0.478245	0.56966	0.604386
261	0.334177	0.335038	0.645719	0.530871	0.614145	0.563964	0.56996	0.604386
262	0.341888	0.349304	0.591443	0.404667	0.478434	0.46391	0.55581	0.674602
263	0.343795	0.338428	0.62232	0.411733	0.604184	0.542539	0.612252	0.719232
264	0.34413	0.343523	0.67819	0.376761	0.665965	0.593117	0.499701	0.411916
265	0.339151	0.341038	0.539536	0.328119	0.443852	0.447153	0.364416	0.359621
266	0.344916	0.324818	0.57288	0.345296	0.447982	0.448722	0.369915	0.359798
267	0.336341	0.331208	0.59151	0.36873	0.461483	0.458152	0.364929	0.34948
268	0.325741	0.335069	0.569331	0.37223	0.474381	0.504154	0.644829	0.352671
269	0.337714	0.320634	0.596309	0.381036	0.461344	0.457443	0.426245	0.384277
270	0.335001	0.321343	0.554085	0.342759	0.446909	0.449654	0.426245	0.384277
271	0.334752	0.334471	0.605433	0.341638	0.478267	0.485296	0.425364	0.407531
272	0.33888	0.336406	0.59254	0.38568	0.731212	0.552823	0.841872	0.938519
273	0.331784	0.330631	0.797536	0.530531	0.646695	0.709115	0.591228	0.585281
274	0.3408	0.320959	0.610766	0.38576	0.455827	0.449733		
275	0.340548	0.351508	0.728537	0.482235				
276	0.334596	0.335368	0.629852	0.387051				
277	0.33457	0.33411	0.54618	0.372055				
278	0.355012	0.328678	0.808849	0.591574				
279	0.356636	0.377239	0.721273	0.552086				
280	0.334135	0.337571	0.666743	0.467571			0.654192	0.651567
281	0.336303	0.33428	0.55408	0.399271			0.379848	0.354203
282	0.321889	0.321161	0.550072	0.353318			0.360529	0.350406
283	0.362742	0.345415	0.601845	0.346499			0.437403	0.474637
284	0.327314	0.336848	0.537261	0.351208			0.481486	0.477917
285	0.321772	0.323756	0.663886	0.40548			0.472783	0.42156
286	0.34126	0.329888	0.597304	0.379546			0.562042	0.434171
287	0.331538	0.325658	0.607956	0.414227			0.429147	0.401485
288	0.325268	0.323315	0.544234	0.325011			0.379748	0.360411
289	0.34427	0.328336	0.553703	0.329511				
290	0.325992	0.327859	0.536697	0.342988				
291	0.333541	0.329913	0.545056	0.322118				
292	0.323605	0.328794	0.571168	0.365241				
293	0.329295	0.324986	0.559489	0.350897			0.364893	0.348916
294	0.336786	0.34186	0.551871	0.320815			0.370115	0.364952
295	0.331154	0.332867	0.54126	0.341595			0.354444	0.347158
296	0.34326	0.324689	0.538638	0.335723			0.371038	0.351097
297	0.323985	0.325363	0.548676	0.353127	0.553119	0.632266	0.384662	0.40121
298	0.323264	0.331596	0.535542	0.341732	0.457212	0.463145	0.375003	0.365356

299	0.324531	0.32638	0.558176	0.358456	0.458216	0.465202	0.365064	0.367101
300	0.328509	0.332514	0.555471	0.330076	0.56075	0.459035	0.372544	0.362114
301	0.323537	0.325476	0.539811	0.334678	0.460705	0.461496	0.379856	0.366519
302	0.33193	0.321061	0.542001	0.33925	0.596186	0.519413	0.408059	0.411275
303	0.32767	0.327169	0.55974	0.350431	0.483347	0.445839	0.483347	0.445839
304	0.323815	0.324286	0.594211	0.425157	0.477184	0.479144	0.447147	0.427728
305	0.325129	0.319818	0.605707	0.429538	0.661486	0.708009	0.504227	0.429751
306	0.345245	0.342064	0.544881	0.373184	0.45674	0.454685	0.392593	0.350692
307	0.330447	0.330581	0.612718	0.410184	0.629573	0.943344	0.365877	0.349701
308	0.325473	0.320329	0.535404	0.34422	0.455223	0.457569	0.360254	0.359374
309	0.326548	0.331774	0.538404	0.370149	0.439256	0.43901	0.391162	0.370795
310	0.330379	0.324071	0.537664	0.404536	0.564262	0.547714	0.489144	0.508196
311	0.3345	0.333124	0.656852	0.413657	0.561133	0.576162	0.484318	0.490082
312	0.339787	0.32564	0.548853	0.375042	0.722509	0.563554	0.364067	0.365358
313	0.334371	0.327516	0.612542	0.444834	0.498521	0.498653		
314	0.327541	0.329929	0.560425	0.385588	0.446798	0.4614	0.375632	0.37177
315	0.321466	0.332477	0.592813	0.394748	0.652016	0.633951	0.453847	0.475992
316	0.321374	0.325607	0.752723	0.387594	0.579153	0.549887	0.494863	0.463792
317	0.324306	0.327379	0.54567	0.370005	0.526222	0.583486	0.367635	0.373776
318	0.318202	0.325144	0.619949	0.36447	0.451994	0.430093	0.384057	0.356327
319	0.329865	0.326247	0.557952	0.365622	0.458233	0.449894	0.357207	0.376614
320	0.326963	0.324722	0.554712	0.336374	0.448752	0.434965	0.3748	0.385961
321	0.333016	0.331038	0.565542	0.347325	0.455635	0.451667	0.363448	0.373267
322	0.325865	0.322434	0.555054	0.333115	0.462071	0.473552	0.350077	0.360369
323	0.333776	0.321686	0.554291	0.338599	0.469528	0.450491	0.37262	0.367438
324	0.342951	0.329682	0.576032	0.352003	0.45186	0.441855	0.36573	0.373946
325	0.328871	0.329014	0.551773	0.346328	0.455563	0.450157	0.402514	0.373941
326	0.333255	0.326169	0.555905	0.327082	0.460888	0.460208	0.366236	0.374691
327	0.325821	0.325026	0.558299	0.338471	0.448849	0.450573	0.371587	0.371465
328	0.335485	0.317444	0.561525	0.319231	0.463125	0.445441	0.371587	0.371465
329	0.325892	0.320123	0.548379	0.340003	0.468697	0.452733	0.365385	0.373452
330	0.328359	0.319137	0.556392	0.337502	0.474264	0.445639	0.360207	0.360405
331	0.327331	0.317048	0.577698	0.355833	0.454679	0.454931	0.360778	0.361563
332	0.324146	0.325532	0.561434	0.327512	0.450406	0.43765	0.366892	0.380317
333	0.335832	0.319374	0.554417	0.352494	0.439992	0.447239	0.363171	0.37238
334	0.327003	0.330515	0.557762	0.332615	0.451018	0.490938	0.394773	0.390527
335	0.322072	0.318905	0.592488	0.344641	0.455144	0.458376	0.38517	0.38295
336	0.329428	0.336884	0.581117	0.373574	0.487803	0.485297	0.380082	0.385621
337	0.343383	0.326454	0.571028	0.334324	0.545495	0.527483	0.368674	0.364437
338	0.335152	0.321326	0.54226	0.35658	0.524984	0.536999	0.372202	0.37819
339	0.326142	0.316634	0.556432	0.348095	0.448306	0.449048	0.367211	0.368119
340	0.324362	0.323547	0.586746	0.336537	0.456691	0.448622	0.367846	0.375336
341	0.342609	0.332343	0.548778	0.324076	0.448326	0.448471	0.378199	0.373874
342	0.343269	0.342112	0.602041	0.380757	0.451335	0.455242	0.377659	0.402133
343	0.325876	0.326017	0.599461	0.378661	0.484288	0.476488	0.380525	0.375159
344	0.33096	0.32207	0.611424	0.36956	0.529441	0.514044	0.484415	0.424017
345	0.329282	0.3383	0.556364	0.321337	0.447475	0.460133	0.371309	0.371506
346	0.33145	0.323194	0.56331	0.336529	0.452664	0.454377	0.36044	0.369368
347	0.340072	0.325822	0.579273	0.322358	0.459612	0.463882	0.36071	0.374285
348	0.32421	0.335421	0.574297	0.386298	0.495658	0.45649	0.399313	0.393869
349	0.348127	0.320254	0.562851	0.331659	0.469712	0.458302	0.36694	0.390021
350	0.338261	0.340636	0.567455	0.361769	0.447431	0.440283	0.372039	0.372149
351	0.334539	0.323836	0.559442	0.33144	0.460747	0.440705	0.37704	0.363108
352	0.330642	0.329608	0.554729	0.33112	0.47681	0.450511	0.393747	0.377428
353	0.321025	0.328224	0.551623	0.347097	0.636529	0.583898	0.503911	0.522293
354	0.345015	0.334805	0.528643	0.322252	0.455259	0.455161	0.373154	0.373522
355	0.325671	0.31843	0.551426	0.327887	0.444333	0.452465	0.38399	0.38965
356	0.33614	0.326445	0.564636	0.327138	0.469298	0.458497	0.389324	0.406259
357	0.345179	0.337199	0.563056	0.354434	0.44464	0.442059	0.375427	0.383666
358	0.333808	0.334499	0.570659	0.352235	0.45934	0.457119	0.361409	0.363875
359	0.325973	0.318299	0.570659	0.341819	0.453835	0.453142	0.359464	0.355847
360	0.334707	0.326447	0.599253	0.346674	0.499637	0.464272	0.380644	0.373568
361	0.321046	0.32541	0.563329	0.348202	0.451613	0.463431	0.367693	0.376852
362	0.33739	0.32813	0.543289	0.331561	0.482587	0.446546	0.382574	0.414735
363	0.320346	0.321989	0.571513	0.373241	0.48018	0.462096	0.369245	0.369469
364	0.340341	0.33901	0.602804	0.359997	0.445101	0.452023	0.358137	0.359477
365			0.564921	0.34207	0.443103	0.440462	0.406493	0.418274



CURRICULUM VITAE

Tuğba KORKMAZ was born in 1992 in ZONGULDAK. She completed her primary, middle and high school educations in Çaycuma city. After completing her high school education in Çaycuma in 2010, she was accepted to Black Sea Technical University in Trabzon. She graduated from her university with an honors degree in 2015. And then she was accepted to Zonguldak Bülent Ecevit University graduate study. She is currently studying on the same program.

ADDRESS:

Address: Hayat Building. Barış Street, No:8/7, Çaycuma/ ZONGULDAK

Phone: (+90) 5541243661

E-mail: korkmztub@gmail.com